

Search for the scalar a_0 and f_0 mesons in the reactions

$$e^+e^- \rightarrow \gamma\pi^0\pi^0(\eta).$$

N.N. Achasov ^{*} and V.V. Gubin [†]

Laboratory of Theoretical Physics

S.L. Sobolev Institute for Mathematics

630090 Novosibirsk 90, Russia

(March 26, 2022)

Abstract

It is shown that the reactions $e^+e^- \rightarrow \gamma\pi^0\pi^0(\eta)$ give a good chance for observing the scalar a_0 and f_0 mesons. In the photon energy region less than 100 MeV the vector meson contributions $e^+e^- \rightarrow V^0 \rightarrow \pi^0 V'^0 \rightarrow \gamma\pi^0\pi^0(\eta)$ are negligible in comparison with the scalar meson $e^+e^- \rightarrow \phi \rightarrow \gamma f_0(a_0) \rightarrow \gamma\pi^0\pi^0(\eta)$ for $BR(\phi \rightarrow \gamma f_0(a_0) \rightarrow \gamma\pi^0\pi^0(\eta))$ greater than $5 \cdot 10^{-6}$ (10^{-5}). Using the two-channel treatment of the $\pi\pi$ scattering the predictions for $BR(\phi \rightarrow \gamma(f_0 + \sigma) \rightarrow \gamma\pi\pi)$ are derived. The four quark model, the model of $K\bar{K}$ molecule and the $s\bar{s}$ model of scalar f_0 and a_0 mesons are discussed.

12.39.-x, 13.40.Hq.

Typeset using REVTeX

^{*}E-mail: achasov@math.nsc.ru

[†]E-mail: gubin@math.nsc.ru

I. INTRODUCTION.

The central problem of light hadron spectroscopy has been the problem of the scalar $f_0(980)$ and $a_0(980)$ mesons. It is well known that these states possess peculiar properties from the naive quark ($q\bar{q}$) model point of view, see, for example, the reviews [1–5]. To clarify the nature of these mesons a number of models has been suggested. It was shown that all their challenging properties could be understood [2,5,6] in the framework of the four-quark ($q^2\bar{q}^2$) MIT-bag model [7], with symbolic quark structure $f_0(980) = s\bar{s}(u\bar{u} + d\bar{d})/\sqrt{2}$ and $a_0(980) = s\bar{s}(u\bar{u} - d\bar{d})/\sqrt{2}$. Along with the $q^2\bar{q}^2$ nature of $a_0(980)$ and $f_0(980)$ mesons the possibility of their being the $K\bar{K}$ molecule is discussed [8].

During the last few years it was established [9–12] that the radiative decays of the ϕ meson $\phi \rightarrow \gamma f_0 \rightarrow \gamma\pi\pi$ and $\phi \rightarrow \gamma a_0 \rightarrow \gamma\eta\pi$ could be a good guideline in distinguishing the f_0 and a_0 meson models. The branching ratios are considerably different in the cases of naive quark, four-quark or molecular models. As has been shown [9], in the four quark model the branching ratio is

$$BR(\phi \rightarrow \gamma f_0(q^2\bar{q}^2) \rightarrow \gamma\pi\pi) \simeq BR(\phi \rightarrow \gamma a_0(q^2\bar{q}^2) \rightarrow \gamma\pi\eta) \sim 10^{-4}, \quad (1)$$

and in the $K\bar{K}$ molecule model it is [10,11]

$$BR(\phi \rightarrow \gamma f_0(K\bar{K}) \rightarrow \gamma\pi\pi) \simeq BR(\phi \rightarrow \gamma a_0(K\bar{K}) \rightarrow \gamma\pi\eta) \sim 10^{-5}. \quad (2)$$

Currently also an interest in an old interpretation of the f_0 meson being an $s\bar{s}$ state, see, [13,14] is rekindled, despite the fact that the almost ideal mass degeneracy of the f_0 and a_0 mesons is difficult to understand in this case. By adding the quark-gluon transitions $q\bar{q} \leftrightarrow gg$ one does not manage this problem. The experiment points rather to the fact that the f_0 meson is weakly coupled with gluons. Really, according QCD [15] we have

$$BR(J/\psi \rightarrow \gamma + gg \text{ in } 0^+ \text{ or } 0^- \text{ states}) = 1,5 \cdot 10^{-2}, \quad (3)$$

but from experiment [16]

$$BR(J/\psi \rightarrow \gamma gg \rightarrow \gamma f_0 \rightarrow \gamma \pi \pi) < 1,4 \cdot 10^{-5} \quad (4)$$

and [17]

$$BR(J/\psi \rightarrow \gamma gg \rightarrow \gamma \eta'(958)) = 4,3 \cdot 10^{-3}. \quad (5)$$

Hence, if one considers that the $\eta'(958)$ coupling with gluons is essential, then the $f_0(980)$ coupling with the gluons should be considered as rather weak.

In spite of this fact, the $s\bar{s}$ scenario is discussed in the current literature as one possible model of the f_0 meson structure. The "accidental" mass degeneracy of a_0 and f_0 mesons in this case is assigned to the final state interaction.

It is easy to note that in the case of an $s\bar{s}$ structure of the f_0 meson $BR(\phi \rightarrow \gamma f_0 \rightarrow \gamma \pi \pi)$ and $BR(\phi \rightarrow \gamma a_0 \rightarrow \gamma \pi \eta)$ are different by factor of ten, which should be visible experimentally. Really, the a_0 meson as an isovector state has a symbolic structure $a_0 = (u\bar{u} - d\bar{d})/\sqrt{2}$ in the two-quark model. In this case the decay $\phi \rightarrow \gamma a_0 \rightarrow \gamma \pi \eta$ is suppressed by the OZI rule and the rough estimation for the real part of the decay amplitude gives [12] $BR(\phi \rightarrow \gamma a_0(q\bar{q}) \rightarrow \gamma \pi \eta) \sim 3 \cdot 10^{-7}$.

By virtue of the real two-particle K^+K^- intermediate state the OZI rule breaking imaginary part of the decay amplitude is relatively high and gives [9]

$$BR(\phi \rightarrow \gamma a_0(q\bar{q}) \rightarrow \gamma \pi \eta) \simeq 5 \cdot 10^{-6}. \quad (6)$$

In the case when $f_0 = s\bar{s}$ the suppression by the OZI rule is absent and the evaluation gives [9]

$$BR(\phi \rightarrow \gamma f_0(s\bar{s}) \rightarrow \gamma \pi \pi) \simeq 5 \cdot 10^{-5}. \quad (7)$$

Let us note that in the case of the $\phi \rightarrow \gamma \eta'$ decay allowed by the OZI rule one expects $BR(\phi \rightarrow \gamma \eta') \simeq 10^{-4}$.

So, the decays $\phi \rightarrow \gamma f_0 \rightarrow \gamma \pi \pi$ and $\phi \rightarrow \gamma a_0 \rightarrow \gamma \pi \eta$ are of special interest for both theorists and the experimentalists.

At the present time the investigation of the $\phi \rightarrow \gamma f_0 \rightarrow \gamma \pi^+ \pi^-$ decay has started with the detector CMD-2 [18] at the e^+e^- -collider VEPP-2M in Novosibirsk. Besides that, in Novosibirsk at the same collider the detector SND has started [19] and has been working with $e^+e^- \rightarrow \gamma f_0 \rightarrow \gamma \pi^0 \pi^0$ and $e^+e^- \rightarrow \gamma a_0 \rightarrow \gamma \eta \pi^0$ decays. The modernization of the VEPP-2M complex is planed to increase the luminosity by one order of magnitude [17]. And, finally, in the near future in Frascati the start of the operation of the ϕ -factory DAΦNE is expected [17], which should make possible extensive studies of the scalar $f_0(980)$ and $a_0(980)$ mesons.

We have shown recently [20] that the search for the f_0 meson in the reaction $e^+e^- \rightarrow \phi \rightarrow \gamma f_0 \rightarrow \gamma \pi^+ \pi^-$ is not an easy task because of the large initial state radiation background. In this paper we study the reactions $e^+e^- \rightarrow \phi \rightarrow \gamma(f_0 + \sigma) \rightarrow \gamma \pi^0 \pi^0$ and $e^+e^- \rightarrow \phi \rightarrow \gamma a_0 \rightarrow \gamma \pi^0 \eta$.

In the second part of the paper, imposing the appropriate photon energy cuts $\omega < 100$ MeV, we show that the background reactions $e^+e^- \rightarrow \rho(\omega) \rightarrow \pi^0 \omega(\rho) \rightarrow \gamma \pi^0 \pi^0$, $e^+e^- \rightarrow \rho(\omega) \rightarrow \pi^0 \omega(\rho) \rightarrow \gamma \pi^0 \eta$ and $e^+e^- \rightarrow \phi \rightarrow \pi^0 \rho \rightarrow \gamma \pi^0 \pi^0(\eta)$ are negligible up to $BR(\phi \rightarrow \gamma f_0(a_0) \rightarrow \gamma \pi^0 \pi^0(\eta), \omega < 100 \text{ MeV}) \sim 5 \cdot 10^{-6}(10^{-5})$. We assume that it will be experimentally possible to isolate photons from $\phi \rightarrow \gamma f_0$ and $\phi \rightarrow \gamma a_0$ with energies $\omega < 100$ MeV, despite the background of the other photons from decays of π^0 and η . This cut plays a strong role in suppression of background, see Sec.II below.

In the third part, basing on a two-channel analysis of the $\pi\pi$ scattering the predictions on $BR(\phi \rightarrow \gamma(f_0 + \sigma) \rightarrow \gamma \pi \pi)$ are made. We discuss the four-quark model of the f_0 and a_0 mesons, the model of the $K\bar{K}$ molecules and the model of the f_0 meson being the $s\bar{s}$ state as well.

The fourth part is devoted to discussions of the obtained results.

II. BACKGROUND TO THE $e^+e^- \rightarrow \gamma f_0(a_0) \rightarrow \gamma \pi^0 \pi^0(\eta)$ REACTION IN THE VECTOR MESON DOMINANCE MODEL.

Let us consider the background to the $e^+e^- \rightarrow \gamma f_0 \rightarrow \gamma \pi^0 \pi^0$ reaction. In the vector meson dominance model the diagrams are pictured in Fig.1. Let us estimate the cross section of the $e^+e^- \rightarrow \rho \rightarrow \pi^0 \omega \rightarrow \pi^0 \pi^0 \gamma$ process, shown in Fig.1(a). First of all, notice that

$$\begin{aligned} \sigma(e^+e^- \rightarrow \rho \rightarrow \pi^0 \omega \rightarrow \pi^0 \pi^0 \gamma, m_\phi) = \\ = \sigma(e^+e^- \rightarrow \rho \rightarrow \pi^0 \omega, m_\phi) \frac{2}{\pi} \int_{m_{min}}^{m_{max}} \frac{m^2 \Gamma_{\omega\pi\gamma}(m) \Lambda_\omega^{3/2} f_\omega(m) dm}{|m_\omega^2 - m^2 - i\Gamma_\omega m|^2}, \end{aligned} \quad (8)$$

where

$$\Gamma_{\omega\pi\gamma}(m) = \Gamma_{\omega\pi\gamma}(m_\omega) \left(\frac{m_\omega}{m} \right)^3 \frac{(m^2 - m_\pi^2)^3}{(m_\omega^2 - m_\pi^2)^3}, \quad \Lambda_\omega = \frac{(m_\phi^2 - (m_\pi - m)^2)(m_\phi^2 - (m_\pi + m)^2)}{(m_\phi^2 - (m_\pi - m_\omega)^2)(m_\phi^2 - (m_\pi + m_\omega)^2)}, \quad (9)$$

and m is the invariant mass of the $\pi\gamma$ system. The limits of the integration are taken with regard to the photon energy cuts $m_{min} \simeq \sqrt{m_\pi^2 + 2m_\pi^2 \omega_{min}/m_\phi} = m_\pi$ and $m_{max} \simeq \sqrt{m_\pi^2 + 2m_\phi \omega_{max}} = 0.471 \text{ GeV}$. The function $f_\omega(m)$ takes into account the interference of the identical pions, see Appendix.

The cross section of the $e^+e^- \rightarrow \rho \rightarrow \pi^0 \omega$ process

$$\sigma(e^+e^- \rightarrow \rho \rightarrow \pi^0 \omega, s) = 12\pi a \frac{\Gamma(\rho \rightarrow e^+e^-, s) \Gamma(\rho \rightarrow \pi^0 \omega, s)}{|D_\rho(s)|^2}, \quad (10)$$

where $\Gamma(\rho \rightarrow e^+e^-, s)$ is defined in Eq.(25) and

$$\Gamma(\rho \rightarrow \pi^0 \omega, s) = \frac{g_{\rho\pi\omega}^2}{96\pi s \sqrt{s}} [(s - (m_\omega - m_\pi)^2)(s - (m_\omega + m_\pi)^2)]^{3/2} \quad (11)$$

The coupling constant $g_{\rho\pi\omega}$ is taken from the width of the decay $\omega \rightarrow \pi\gamma$ data that leads to $g_{\rho\pi\omega}^2/96\pi = 0.452 \text{ GeV}^{-2}$. In the propagator D_ρ we are taking into account the energy dependence of the ρ meson width

$$D_\rho(s) = m_\rho^2 - s - is \frac{g_{\rho\pi\pi}^2}{48\pi} \left(1 - \frac{4m_\pi^2}{s}\right)^{3/2}. \quad (12)$$

The constant a is taken from the condition $\sigma(e^+e^- \rightarrow \pi^0\omega, \sqrt{s} = 0.97) = 6.1$ nb, see [21], that leads to $a = 2.02$.

From the above, the cross section $\sigma(e^+e^- \rightarrow \rho \rightarrow \pi^0\omega, m_\phi) = 6.46$ nb. The cross section of the $e^+e^- \rightarrow \rho \rightarrow \pi^0\omega \rightarrow \pi^0\pi^0\gamma$ process is

$$\sigma(e^+e^- \rightarrow \rho \rightarrow \pi^0\omega \rightarrow \pi^0\pi^0\gamma, m_\phi) = 6.1 \cdot 10^{-4} \text{ nb.} \quad (13)$$

in the region of interest $0 < \omega < 100$ MeV. Analogously let us consider the $e^+e^- \rightarrow \omega \rightarrow \pi^0\rho \rightarrow \gamma\pi^0\pi^0$ process, see Fig.1(b). First, we have

$$\begin{aligned} \sigma(e^+e^- \rightarrow \omega \rightarrow \pi^0\rho \rightarrow \pi^0\pi^0\gamma, m_\phi) = \\ = \sigma(e^+e^- \rightarrow \omega \rightarrow \pi^0\rho, m_\phi) \frac{2}{\pi} \int_{m_{min}}^{m_{max}} \frac{m^2 \Gamma_{\rho\pi^0\gamma}(m) \Lambda_\rho^{3/2} f_\rho(m) dm}{|D_\rho(m)|^2}, \end{aligned} \quad (14)$$

where

$$\Gamma_{\rho\pi^0\gamma}(m) = \Gamma_{\rho\pi^0\gamma}(m_\rho) \left(\frac{m_\rho}{m} \right)^3 \frac{(m^2 - m_\pi^2)^3}{(m_\rho^2 - m_\pi^2)^3}, \quad \Lambda_\rho = \frac{(m_\phi^2 - (m_\pi - m)^2)(m_\phi^2 - (m_\pi + m)^2)}{(m_\phi^2 - (m_\pi - m_\rho)^2)(m_\phi^2 - (m_\pi + m_\rho)^2)}. \quad (15)$$

The cross section of the $e^+e^- \rightarrow \omega \rightarrow \pi^0\rho^0$ process is

$$\sigma(e^+e^- \rightarrow \omega \rightarrow \pi^0\rho, s) = 12\pi b \frac{\Gamma(\omega \rightarrow e^+e^-, s) \Gamma(\omega \rightarrow \pi^0\rho, s)}{|D_\omega(s)|^2}. \quad (16)$$

The constant b is found from the condition $\sigma(e^+e^- \rightarrow \omega \rightarrow \pi^0\pi^+\pi^-; \sqrt{s} = 1.09) \simeq \sigma(e^+e^- \rightarrow \omega \rightarrow \pi^0\rho; \sqrt{s} = 1.09) \simeq 2.4$ nb, see [21], that leads to $b = 4.7$. In view of it the cross section $\sigma(e^+e^- \rightarrow \omega \rightarrow \pi^0\rho; m_\phi) \simeq 2.2$ nb. For the cross section of the $e^+e^- \rightarrow \omega \rightarrow \pi^0\rho \rightarrow \gamma\pi^0\pi^0$ process in the photon energy region $0 < \omega < 100$ MeV, see (14), one has

$$\sigma(e^+e^- \rightarrow \omega \rightarrow \pi^0\rho \rightarrow \gamma\pi^0\pi^0, m_\phi) = 3.2 \cdot 10^{-5} \text{ nb.} \quad (17)$$

The cross section of the $e^+e^- \rightarrow \phi \rightarrow \pi^0\rho^0 \rightarrow \gamma\pi^0\pi^0$ process, see Fig.1(c), in the ϕ meson region at $0 < \omega < 100$ MeV is

$$\begin{aligned}
& \sigma(e^+e^- \rightarrow \phi \rightarrow \pi^0 \rho \rightarrow \gamma \pi^0 \pi^0, m_\phi) = \\
& = \sigma(e^+e^- \rightarrow \phi \rightarrow \pi^0 \rho, m_\phi) \frac{2}{\pi} \int_{m_{min}}^{m_{max}} \frac{m^2 \Gamma_{\rho \pi^0 \gamma}(m) \Lambda_\rho^{3/2} f_\rho(m) dm}{|D_\rho(m)|^2} < 2.6 \cdot 10^{-3} \text{ nb},
\end{aligned} \tag{18}$$

where $BR(\phi \rightarrow \pi^0 \rho^0 \rightarrow \gamma \pi^0 \pi^0, \omega < 100 \text{ MeV}) < 6.4 \cdot 10^{-7}$ ¹.

In principle, the interference between the amplitudes $e^+e^- \rightarrow V \rightarrow \gamma V' \rightarrow \gamma \pi^0 \pi^0$ may be essential, but, as it is seen from Eq.(13), Eq.(17) and Eq.(18), in studies of the background to the $e^+e^- \rightarrow \gamma f_0 \rightarrow \gamma \pi^0 \pi^0$ reaction one can neglect the contributions of the $e^+e^- \rightarrow \rho(\omega) \rightarrow \pi^0 \omega(\rho) \rightarrow \pi^0 \pi^0 \gamma$ processes and the question of their interference no longer arises.

Hence, taking into account that $\sigma(e^+e^- \rightarrow \phi \rightarrow \text{all}) = 4.4 \cdot 10^3 \text{ nb}$, the background processes $e^+e^- \rightarrow V^0 \rightarrow \pi^0 V^0 \rightarrow \gamma \pi^0 \pi^0$ are negligible compared to the one under study $e^+e^- \rightarrow \gamma f_0 \rightarrow \gamma \pi^0 \pi^0$ up to $BR(\phi \rightarrow \gamma f_0 \rightarrow \gamma \pi^0 \pi^0) = 5 \cdot 10^{-6}$ ².

As for the interference between the primary process $e^+e^- \rightarrow \gamma f_0 \rightarrow \gamma \pi^0 \pi^0$ and the background process $e^+e^- \rightarrow \phi \rightarrow \pi^0 \rho \rightarrow \gamma \pi^0 \pi^0$, one can neglect it also due to the fact that 66% of background contribution to the branching ratio under consideration is determined by the region $70 < \omega < 100 \text{ MeV}$ while the contribution of the primary process in this region is less than 20% in the worst case when the f_0 meson is relatively wide, see Sec.IV.

Let us consider the background to the $e^+e^- \rightarrow \gamma a_0 \rightarrow \gamma \pi^0 \eta$ reaction. It is easy to show that in this case, as in the case of the reaction $e^+e^- \rightarrow \gamma f_0 \rightarrow \gamma \pi^0 \pi^0$, the process $e^+e^- \rightarrow \phi \rightarrow \pi^0 \rho \rightarrow \gamma \pi^0 \eta$ is dominant. The cross sections of the processes $e^+e^- \rightarrow \rho(\omega) \rightarrow \eta \rho(\omega) \rightarrow \gamma \pi^0 \eta$, see Fig.2, are by two orders of magnitude less than the cross sections of the processes $e^+e^- \rightarrow \rho(\omega) \rightarrow \pi^0 \omega(\rho) \rightarrow \gamma \pi^0 \eta$. The cross sections of the processes $e^+e^- \rightarrow \rho(\omega) \rightarrow \pi^0 \omega(\rho) \rightarrow \gamma \pi^0 \eta$, in turn, are by two orders of magnitude less than the cross section of the process $e^+e^- \rightarrow \phi \rightarrow \pi^0 \rho \rightarrow \gamma \pi^0 \eta$. In comparison with the process $e^+e^- \rightarrow \phi \rightarrow \pi^0 \rho \rightarrow \gamma \pi^0 \eta$ the cross section of the process $e^+e^- \rightarrow \phi \rightarrow \eta \phi \rightarrow \gamma \pi^0 \eta$ is

¹ Taking into account the positive interference one has $BR(\phi \rightarrow \pi^0 \rho^0) < (1/3)BR(\phi \rightarrow \pi \rho)$.

² Let us emphasize that we essentially use the photon energy cuts in our analyses. For comparison we notice that after integration over all spectrum $BR(\phi \rightarrow \pi^0 \rho^0 \rightarrow \gamma \pi^0 \pi^0) \simeq 10^{-5}$ [9,22–24].

suppressed by two orders of magnitude also.

The cross section of the process $e^+e^- \rightarrow \phi \rightarrow \pi^0 \rho \rightarrow \gamma \pi^0 \eta$

$$\begin{aligned} \sigma(e^+e^- \rightarrow \phi \rightarrow \pi^0 \rho \rightarrow \pi^0 \eta \gamma, m_\phi) = \\ = \sigma(e^+e^- \rightarrow \phi \rightarrow \pi^0 \rho, m_\phi) \frac{2}{\pi} \int_{m_{min}}^{m_{max}} \frac{m^2 \Gamma_{\rho\eta\gamma}(m) \Lambda_\rho^{3/2} dm}{|D_\rho|^2}. \end{aligned} \quad (19)$$

Let us take into account that

$$\frac{2}{\pi} \int_{m_{min}}^{m_{max}} \frac{m^2 \Gamma_{\rho\eta\gamma}(m) \Lambda_\rho^{3/2} dm}{|D_\rho|^2} = 3.5 \cdot 10^{-5}, \quad (20)$$

where

$$\Gamma_{\rho\eta\gamma}(m) = \Gamma_{\rho\eta\gamma}(m_\rho) \left(\frac{m_\rho}{m} \right)^3 \frac{(m^2 - m_\eta^2)^3}{(m_\rho^2 - m_\eta^2)^3}, \quad (21)$$

and m is the invariant mass of the $\eta\gamma$ system. The integration limits are taken with regard to the photon energy cuts $m_{min} \simeq \sqrt{m_\eta^2 + 2m_\pi^2 \omega_{min}/m_\phi} = m_\eta$ and $m_{max} \simeq \sqrt{m_\eta^2 + 2m_\phi \omega_{max}} = 0.71 \text{ GeV}$.

Taking into account that $\sigma(e^+e^- \rightarrow \phi \rightarrow \pi^0 \rho, m_\phi) < 182 \text{ nb}$, for the cross section of the process $e^+e^- \rightarrow \phi \rightarrow \pi^0 \rho \rightarrow \pi^0 \eta \gamma$ in the region $\omega < 100 \text{ MeV}$ one gets

$$\sigma(e^+e^- \rightarrow \phi \rightarrow \pi^0 \rho \rightarrow \pi^0 \eta \gamma, m_\phi) < 6.37 \cdot 10^{-3} \text{ nb}, \quad (22)$$

wich corresponds to $BR(\phi \rightarrow \pi^0 \rho^0 \rightarrow \gamma \pi^0 \eta, \omega < 100 \text{ MeV}) < 1.5 \cdot 10^{-6}$.

So, the processes $e^+e^- \rightarrow V^0 \rightarrow \pi^0 V'^0 \rightarrow \gamma \pi^0 \eta$ and $e^+e^- \rightarrow V^0 \rightarrow \eta V'^0 \rightarrow \gamma \pi^0 \eta$ which are the background to $e^+e^- \rightarrow \gamma a_0 \rightarrow \gamma \pi^0 \eta$ are negligible for $BR(\phi \rightarrow \gamma a_0 \rightarrow \gamma \pi^0 \eta)$ greater than 10^{-5} .

As for the interference between the $e^+e^- \rightarrow \gamma a_0 \rightarrow \gamma \pi^0 \eta$ and $e^+e^- \rightarrow \phi \rightarrow \pi^0 \rho \rightarrow \gamma \pi^0 \eta$ processes, one can neglect it also due to the fact that 80% of background contribution to the branching ratio under consideration is determined by the region $70 < \omega < 100 \text{ MeV}$ while the contribution of the primary process in this region is less than 20% in the worst case when the a_0 meson is relatively wide, see Sec.IV.

Notice that if it should be possible to choose a cut on photon energy $\omega < 50 \text{ MeV}$ the background would be one order of magnitude less than previously stated while the primary processes $e^+e^- \rightarrow \phi \rightarrow \gamma f_0(a_0) \rightarrow \gamma \pi^0 \pi^0(\eta)$ would not decrease considerably.

III. MIXING f_0 AND σ MESONS.

A. $q^2\bar{q}^2$ and $q\bar{q}$ models.

The background from processes $e^+e^- \rightarrow V^0 \rightarrow \pi^0 V^0 \rightarrow \gamma\pi^0\pi^0(\eta)$ described above are negligible up to $BR(\phi \rightarrow \gamma\pi^0\pi^0(\eta), \omega < 100 \text{ MeV}) = 5 \cdot 10^{-6}(10^{-5})$. In the meantime the one-loop calculation in the frame of the chiral perturbation theory of $BR(\phi \rightarrow \gamma K\bar{K} \rightarrow \gamma\pi\pi(\eta))$ at $\omega < 100 \text{ MeV}$ leads to the number of 10^{-5} order of magnitude, see [25]. So, in such a theory the strong interference effects with the reaction $\phi \rightarrow \gamma f_0(a_0) \rightarrow \gamma\pi\pi(\eta)$ are predicted. But one cannot restrict oneself to the one-loop approximation only in the region discussed ($\sim 1 \text{ GeV}$), see, for example, [26]. In view of the fact that all the corrections to the amplitude in the chiral model cannot be taken into account, we treat them in the phenomenological way considering the scalar particle called σ meson that is strongly coupled with $\pi\pi$ channel and, in view of mixing with f_0 meson, can change considerably the photon energy differential cross section. The parameters of the σ meson we obtain from fitting the $\pi\pi$ scattering data.

Let us consider the reaction $e^+e^- \rightarrow \phi \rightarrow \gamma(f_0 + \sigma) \rightarrow \gamma\pi^0\pi^0$ with regard to the mixing of the f_0 and σ mesons. Below is the formalism in the frame of which we study this problem.

We consider the one loop mechanism of the R meson production, where $R = f_0, \sigma$, through the charged kaon loop, $\phi \rightarrow K^+K^- \rightarrow \gamma R$, see [9–12]. The symbolic diagram is shown in Fig.3(a). The amplitude $\phi \rightarrow \gamma R$ in the rest frame of the ϕ meson is parametrized in the following manner

$$M = g(m)g_{RK^+K^-}\vec{e}(\phi)\vec{e}(\gamma) \quad (23)$$

where $m^2 = (k_1 + k_2)^2 = s - 2\sqrt{s}\omega$ is the invariant mass of the $\pi\pi$ system, $\vec{e}(\phi)$ and $\vec{e}(\gamma)$ are the polarization vectors of the ϕ meson and photon respectively. The expression of the $g(m)$ function obtained in the four-quark ($q^2\bar{q}^2$) model is written down in [9].³

³ For a convenience, in this paper, we use a different parametrization of the amplitude (23).

Notice that in the four-quark and two-quark models the scalar mesons are considered to be point like objects [9,12] but in the model of the $K\bar{K}$ molecule they are considered as extended ones [8].

Taking into account the mixing of the f_0 and σ mesons, the amplitude of the reaction $e^+(p_1)e^-(p_2) \rightarrow \phi \rightarrow \gamma(f_0 + \sigma) \rightarrow \gamma(q)\pi^0(k_1)\pi^0(k_2)$ is written in the following way [2,27]

$$M = e\bar{u}(-p_1)\gamma^\mu u(p_2)\frac{em_\phi^2}{f_\phi}\frac{e^{i\delta_B}}{sD_\phi(s)}g(m)(e(\gamma)^\mu - q^\mu\frac{e(\gamma)p}{pq})\sum_{RR'}(g_{RK^+K^-}G_{RR'}^{-1}(m)g_{R'\pi^0\pi^0}) \quad (24)$$

where $s = p^2 = (p_1 + p_2)^2$, $g_R(m) \sim (pq) \rightarrow 0$ at $(pq) \rightarrow 0$ and δ_B is the phase of the elastic background, see (41). The constant f_ϕ is related to the electron width of the vector meson decay

$$\Gamma(V \rightarrow e^+e^-, s) = \frac{4\pi\alpha^2}{3}\left(\frac{m_V^2}{f_V}\right)^2\frac{1}{s\sqrt{s}} \quad (25)$$

For the differential cross section one gets

$$\frac{d\sigma_\phi}{d\omega} = \frac{\alpha^2\omega}{8\pi s^2}\left(\frac{m_\phi^2}{f_\phi}\right)^2\frac{|g(m)|^2}{|D_\phi(s)|^2}\sqrt{1 - \frac{4m_\pi^2}{m^2}}\left(c + \frac{c^3}{3}\right)\left|\sum_{RR'}(g_{RK^+K^-}G_{RR'}^{-1}g_{R'\pi^0\pi^0})\right|^2 H(s, \omega_{min}) \quad (26)$$

where $\omega = |\vec{q}|$ is the energy of the photon, c is the cut on $\cos\theta_\gamma$, where θ_γ is the angle between the photon momentum direction and the beam in the center of mass frame of the considered reaction: $-c \leq \cos\theta_\gamma \leq c$. The function $H(s, \omega_{min})$ takes into account the radiative corrections, the contribution of which is about 20% [28].

$$H(s, \omega_{min}) = \frac{1}{|1 - \Pi(s)|^2}\left\{1 + \frac{2\alpha}{\pi}[(L - 1)\ln\frac{2\omega_{min}}{\sqrt{s}} + \frac{3}{4}L + \frac{\pi^2}{6} - 1]\right\} \quad (27)$$

where ω_{min} is the minimal photon energy registered in the experiment, $L = \ln\frac{s}{m_e^2}$ is the "main" logarithm. The electron vacuum polarization to the one order of α is

$$\Pi(s) = \frac{\alpha}{3\pi}(L - \frac{5}{3}), \quad (28)$$

the contribution of the muon and light hadron has been omitted. Describing the photon spectrum, we shall use the photon energy cuts $20 < \omega < 100$ MeV that allows the separation of the signal from the other states contributing in the differential cross section. But,

Please, compare with [9,11,12,20]

calculating the branching ratios of the processes, we shall neglect the ω_{min} , as it was done above, and use the photon energy cut $\omega < 100$ MeV.

The matrix of the inverse propagator has the form

$$G_{RR'}(m) = \begin{pmatrix} D_{f_0}(m) & -\Pi_{f_0\sigma}(m) \\ -\Pi_{\sigma f_0}(m) & D_{\sigma}(m) \end{pmatrix}$$

For the propagator of the scalar particle we use the following expression

$$D_R(m) = m_R^2 - m^2 + \sum_{ab} g_{Rab} [Re P_R^{ab}(m_R^2) - P_R^{ab}(m)], \quad (29)$$

where $\sum_{ab} g_{Rab} [Re P_R^{ab}(m_R^2) - P_R^{ab}(m)] = \Pi_R(m) = \Pi_{RR}(m)$ takes into account the finite width corrections of the resonance which are the one loop contribution to the self-energy of the R resonance from the two-particle intermediate ab states. In the $q^2\bar{q}^2$ model of the scalar particle and in the model of the $K\bar{K}$ molecule the f_0 and a_0 mesons are strongly coupled with the $K\bar{K}$ channel, since they are just under the threshold of this channel. The ordinary resonance expression of the propagator, in view of this coupling, is changed considerably and the account of $\sum_{ab} g_{Rab} [Re P_R^{ab}(m_R^2) - P_R^{ab}(m)]$ corrections is necessary, see [2,9,11,29]. Notice that the expression (26) for mixing of the f_0 and σ mesons takes into account the all order of the perturbation theory, the symbolic diagrams are shown in Fig.3.

For the pseudoscalar ab mesons and $m_a \geq m_b$, $m^2 > m_+^2$ one has

$$P_R^{ab}(m) = \frac{g_{Rab}}{16\pi} \left[\frac{m_+ m_-}{\pi m^2} \ln \frac{m_b}{m_a} + \rho_{ab} \left(i + \frac{1}{\pi} \ln \frac{\sqrt{m^2 - m_-^2} - \sqrt{m^2 - m_+^2}}{\sqrt{m^2 - m_-^2} + \sqrt{m^2 - m_+^2}} \right) \right] \quad (30)$$

In other regions of m one can obtain the $P_R^{ab}(m)$ by analytical continuation of Eq.(30), see [12,20,30].

The constants g_{Rab} are related to the width

$$\Gamma(R \rightarrow ab, m) = \frac{g_{Rab}^2}{16\pi m} \rho_{ab}(m), \quad (31)$$

where $\rho_{ab}(m) = \sqrt{(m^2 - m_+^2)(m^2 - m_-^2)}/m^2$ and $m_{\pm} = m_a \pm m_b$.

Nondiagonal elements of the matrix $G_{RR'}(m)$ are the transitions caused by the resonance mixing due to the final state interaction which occurred in the same decay channels $R \rightarrow (ab) \rightarrow R'$. We write them down in the following manner [2,27]

$$\Pi_{RR'}(m) = \sum_{ab} g_{R'ab} P_R^{ab}(m) + C_{RR'}, \quad (32)$$

where the constants $C_{RR'}$ take into account effectively the contribution of VV , $4P$ and other intermediate states and incorporate the subtraction constants for the $R \rightarrow (PP) \rightarrow R'$ transitions. In the four-quark and two-quark models we treat these constants as a free parameters.

B. Model of $K\bar{K}$ molecule.

The model of the $K\bar{K}$ molecule was formulated in [8] and developed in the papers [10,11], as applied to the $\phi \rightarrow \gamma f_0(a_0) \rightarrow \gamma \pi \pi(\eta)$ decay.

A specific feature of the molecular model is the narrow structure of the f_0 and a_0 mesons.

Really, the width of the weakly bound, quasi-stable system cannot be larger than the bound energy which is $\epsilon = 10 - 20$ MeV for the $K\bar{K}$ mesons, see, for example, [8]. So, in the molecular model the effective width of the f_0 and a_0 mesons is $\Gamma_{eff} < 20$ MeV. The $\pi\pi$ scattering data, as we shall see below, permit the width of the f_0 meson to be $\Gamma_{eff} = 0.01 - 0.03$ GeV. Such widths, with some stretch of the interpretation ⁴ can be associated with the $K\bar{K}$ bound state. But, nevertheless, we suppose that the latest experimental data are difficult (apparently impossible) to understand in the framework of this model as they point to the rather wide f_0 resonance with the $\Gamma_{eff} \sim 40 - 100$ MeV, see [31–33,41]. The objections against the $K\bar{K}$ bound state interpretation were also presented in [34]. As for the a_0 resonance, it seemed to be always too wide for a such interpretation, $\Gamma_{eff} \sim 50 - 100$ MeV, see [36]. The latest data confirm this. The a_0 meson with the $\Gamma_{eff} \simeq 90 \pm 11$ MeV was observed in the reaction $\pi^- p \rightarrow \pi^0 \eta n$ (Brookhaven), see [33].

In the model of the scalar $K\bar{K}$ molecule [10] the function $g(m)$ was calculated in [11]. In this paper it was found that the imaginary part of the $\phi \rightarrow \gamma f_0$ amplitude gives 90% of $BR(\phi \rightarrow \gamma f_0 \rightarrow \gamma \pi \pi)$. In view of this, we take into account only the imaginary part of the

⁴ Strictly speaking, the width should be much less then the bound energy.

$g(m)$. In the transitions caused by the resonance mixing due to the final state interaction only real intermediate states are involved (the virtual states are suppressed for an extended molecule). Because of virtual states suppression, we write in the model of $K\bar{K}$ molecule the nondiagonal elements of the inverse propagator matrix in the following way

$$\Pi_{RR'}(m) = Im \sum_{ab} g_{R'ab} P_R^{ab}(m). \quad (33)$$

As for the propagator of the f_0 meson, let us take the generally accepted Breit - Wigner formulae.

When $m > 2m_{K^+} \ 2m_{K^0}$,

$$\begin{aligned} D_{f_0}(m) &= M_{f_0}^2 - m^2 - i(\Gamma_0(m) + \Gamma_{K\bar{K}}(m))m \\ \Gamma_{K\bar{K}}(m) &= \frac{g_{f_0 K^+ K^-}^2}{16\pi} (\sqrt{1 - 4m_{K^+}^2/m^2} + \sqrt{1 - 4m_{K^0}^2/m^2}) \frac{1}{m} . \end{aligned} \quad (34)$$

As a parameter of the model we use the decay width $\Gamma(f_0(a_0) \rightarrow \pi\pi(\eta)) = \Gamma_0$ which is defined in Eq.(31). In other areas of m one can obtain the $D_{f_0}(m)$ by analytical continuation of Eq.(34), see [11,29].

Since the scalar resonances lie under the $K\bar{K}$ thresholds the position of the peak in the cross section or in the mass spectrum does not coincide with M_{f_0} , as one can see from analytical continuation of Eq.(34) under the $K\bar{K}$ threshold [11,29]. That is why it is necessary to renormalize the mass in the Breit - Wigner formulae

$$M_{f_0}^2 = m_R^2 - \frac{g_{f_0 K^+ K^-}^2}{16\pi} (\sqrt{4m_{K^+}^2/m_{f_0}^2 - 1} + \sqrt{4m_{K^0}^2/m_{f_0}^2 - 1}) , \quad (35)$$

where $m_{f_0}^2$ is the physical mass squared ($m_{a_0} = 980$ MeV and $m_{f_0} = 980$ MeV) while $M_{f_0}^2$ is the bare mass squared. So, the physical mass is heavier than the bare one. This circumstance is especially important in the case of a strong coupling of the scalar mesons with the $K\bar{K}$ channel as in the molecular models.

In the molecular model the coupling constant of the f_0 meson with the $K\bar{K}$ channel is [10]

$$\frac{g_{f_0 K^+ K^-}^2}{4\pi} = 0.6 \text{ GeV}^2. \quad (36)$$

Notice that in this model $m_{f_0} - M_{f_0} = 24(10)$ MeV for $m_{f_0} = 980(2m_{K^+})$. The value of Γ_0 is fixed in the region $0.05 - 0.1$ GeV that leads, on average, to the effective widths $\Gamma_{eff} \simeq 0.01 - 0.03$ GeV.

C. Analyses of data on the $\pi\pi \rightarrow \pi\pi$ scattering.

To fit the $\pi\pi$ scattering data we write the s -wave amplitude of the $\pi\pi \rightarrow \pi\pi$ reaction with $I = 0$ as the sum of the inelastic resonance amplitude $T_{\pi\pi}^{res}$, in which the contributions of the f_0 and σ mesons are taken onto account, and the amplitude of the elastic background [2,27]

$$T(\pi\pi \rightarrow \pi\pi) = \frac{\eta_0^0 e^{2i\delta_0^0} - 1}{2i\rho_{\pi\pi}} = \frac{e^{2i\delta_B} - 1}{2i\rho_{\pi\pi}} + e^{2i\delta_B} T_{\pi\pi}^{res}, \quad (37)$$

where

$$T_{\pi\pi}^{res} = \sum_{RR'} \frac{g_{R\pi\pi} g_{R'\pi\pi}}{16\pi} G_{RR'}^{-1}(m) \quad (38)$$

The elastic background phase δ_B is taken in the form $\delta_B = \theta\rho_{\pi\pi}(m)$, where $\theta \sim 60^\circ$. The expressions like Eq.(37) are commonly used for the fitting in the wide energy region. This fairly simple approximation works to advantage in the f_0 resonance region both in the $\pi\pi \rightarrow \pi\pi$ and in the $\pi\pi \rightarrow K\bar{K}$ reactions. The $\pi\pi \rightarrow K\bar{K}$ channel is the first important inelastic channel of the $\pi\pi$ scattering in the s -wave. Defying the relations

$$\begin{aligned} g_{f_0 K\bar{K}} &= \sqrt{2}g_{f_0 K^+ K^-} = \sqrt{2}g_{f_0 K^0 \bar{K}^0} \\ g_{\sigma K\bar{K}} &= \sqrt{2}g_{\sigma K^+ K^-} = \sqrt{2}g_{\sigma K^0 \bar{K}^0}, \end{aligned} \quad (39)$$

we get for inelasticity the following expression

$$\begin{aligned} \eta_0^0 &= 1; \quad m < 2m_{K^+} \\ \eta_0^0 &= \sqrt{1 - 2\rho_{\pi\pi}(m)\rho_{K^+ K^-}(m)|T_{K\bar{K}}|^2}; \quad 2m_{K^+} < m < 2m_{K^0} \\ \eta_0^0 &= \sqrt{1 - 2\rho_{\pi\pi}(m)(\rho_{K^+ K^-}(m) + \rho_{K^0 \bar{K}^0}(m))|T_{K\bar{K}}|^2}; \quad m > 2m_{K^0} \end{aligned} \quad (40)$$

where the amplitude of the $\pi\pi \rightarrow K\bar{K}$ process is

$$T_{K\bar{K}} = e^{i\delta_B} \sum_{RR'} \frac{g_{R\pi\pi} g_{R'K\bar{K}}}{16\pi} G_{RR'}^{-1}(m). \quad (41)$$

IV. RESULTS AND DISCUSSIONS.

A. $f_0(980)$ resonance.

In the four-quark model we consider the following parameters as free: the coupling constant of the f_0 meson to the $K\bar{K}$ channel $g_{f_0 K^+ K^-}$, the coupling constant of the σ meson to the $\pi\pi$ channel $g_{\sigma\pi\pi}$, the constant $C_{f_0\sigma}$, the ratio $R = g_{f_0 K^+ K^-}^2 / g_{f_0 \pi^+ \pi^-}^2$, the phase θ of the elastic background and the σ meson mass. The mass of the f_0 meson is restricted to the region $0.97 < m_{f_0} < 0.99$ GeV. We treat the σ meson as an ordinary two-quark state the coupling constant of which with the $K\bar{K}$ channel must be related in the naive quark model to the constant $g_{\sigma\pi\pi}$. One gets $g_{\sigma K^+ K^-} = g_{\sigma\pi^+ \pi^-} / 2$. From the analyses of the radiative decays of the J/ψ meson it is evident that the strange quark production is suppressed by a factor of $\lambda \simeq 1/2$ in comparison with u and d quarks [35]

$$u\bar{u} : d\bar{d} : s\bar{s} = 1 : 1 : \lambda \quad (42)$$

This leads to the additional suppression of the coupling constant of the σ meson with the $K\bar{K}$ channel, $g_{\sigma K^+ K^-} = \sqrt{\lambda} g_{\sigma\pi^+ \pi^-} / 2 \simeq 0.35 g_{\sigma\pi^+ \pi^-}$. As it was found, the fitting depends on the constant $g_{\sigma K^+ K^-}$ very weakly and we drop this constant. We do not consider the coupling of the σ meson with the $\eta\eta$ channel as well. In the naive quark model this coupling is relatively suppressed. If the angle of the $\eta - \eta'$ mixing is chosen to be $\theta_{\eta\eta'} = -18^\circ$ one gets $g_{\sigma\eta\eta} \simeq (\sqrt{2}/3) g_{\sigma\pi^+ \pi^-}$.

We use the data presented in the papers [37,38] for the fitting of the phase δ_0^0 of the $\pi\pi$ scattering and the data presented in the papers [37,39] for fitting the inelasticity η_0^0 .

The fitting shows that in the four quark model a number of parameters describe well enough the $\pi\pi$ scattering in the region $0.7 < m < 1.8$ GeV. Our results in the $(q^2 \bar{q}^2)$ model are tabulated in the Table I. In this table the following parameters and predictions are listed:

the effective widths of the f_0 meson Γ_{eff} , the branching ratios $BR_{f_0+\sigma}(BR_{f_0}) = 3 \cdot BR(\phi \rightarrow \gamma(f_0 + \sigma) \rightarrow \gamma\pi^0\pi^0)(3 \cdot BR(\phi \rightarrow \gamma f_0 \rightarrow \gamma\pi^0\pi^0))$ of the decays $\phi \rightarrow \gamma(f_0 + \sigma) \rightarrow \gamma\pi\pi$ and $\phi \rightarrow \gamma f_0 \rightarrow \gamma\pi\pi$ integrated over the range $0.7 < m < m_\phi$ (corresponding to $\omega < 250$ MeV) and taking into account the energy cut $\omega < 100$ GeV (the range $0.9 < m < m_\phi$)⁵. Besides that we study the dependence of the fitting parameters on the mass of the f_0 meson. All dimensional quantities in the tables are presented in the units of GeV or in GeV^2 . The picture for one set of the parameters is shown in Fig 4.

As it is seen from the Table I, one can change the effective width of the f_0 meson from the very narrow $\Gamma_{eff} \simeq 10$ MeV to the relatively wide $\Gamma_{eff} \simeq 100$ MeV, varying the parameters in the four-quark model. The parameters of the σ meson are approximately unchanged $m_\sigma \simeq 1.48$ GeV, $g_{\sigma\pi\pi}^2/4\pi \simeq 1.8$ GeV^2 . The decay width of the σ meson to 2π is $\Gamma_{2\pi}(m_\sigma) \simeq 300$ MeV. Besides, it is seen that in spite of the f_0 and σ mixing the branching ratios of the decays $\phi \rightarrow \gamma f_0 \rightarrow \gamma\pi\pi$ and $\phi \rightarrow \gamma(f_0 + \sigma) \rightarrow \gamma\pi\pi$ are approximately the same and have the order of 10^{-4} .

Recall that in the four-quark model the coupling of the a_0 and f_0 states to the $K\bar{K}$ channel is strong, superallowed by OZI rule [7,2], $g_{f_0(a_0)}^2/4\pi \gtrsim 1$ GeV^2 . Besides, in the $q^2\bar{q}^2$ model, where the f_0 meson has a symbolic structure $f_0 = s\bar{s}(u\bar{u}+d\bar{d})/\sqrt{2}$, the coupling of the f_0 meson to the $\pi\pi$ channel is relatively suppressed. In this case one should consider $R = 1, 2$ as a relative enhancement since the comparison should be made with $R = g_{f_0K^+K^-}^2/g_{f_0\pi^+\pi^-}^2 = \lambda/4 = 1/8$ in the case of $f_0 = (u\bar{u} + d\bar{d})/\sqrt{2}$.

The three last lines in Table I are devoted to the $s\bar{s}$ model of the f_0 meson. In such a model the f_0 meson is considered as a point-like object, i.e. in the $K\bar{K}$ loop, $\phi \rightarrow K^+K^- \rightarrow \gamma f_0$ and in the transitions caused by the resonance mixing we consider both the real and the virtual intermediate states. It is typical for the $s\bar{s}$ model of the f_0 meson that the coupling with the $\pi\pi$ channel is relatively suppressed. In this sense this model is different from the $q^2\bar{q}^2$

⁵ Notice that $BR(\phi \rightarrow \gamma\pi^0\pi^0) = (1/3)BR(\phi \rightarrow \gamma\pi\pi)$.

model by the small coupling constant $g_{f_0 K^+ K^-}$ only, in the $s\bar{s}$ model $g_{f_0 K^+ K^-}^2/4\pi \sim 0.3 \text{ GeV}^2$. The small coupling constant $g_{f_0 K^+ K^-}$ arises from the requirement of the relation between constants $g_{a_0 \pi \eta}$ and $g_{f_0 K^+ K^-}$ in the two-quark model. If the angle of the $\eta - \eta'$ mixing is chosen to be $\theta_{\eta\eta'} = -18^\circ$ one gets $g_{a_0 \pi \eta} = 2 \cos(\theta_{\eta\eta'} + \theta_p) g_{a_0 K^+ K^-} = 1.6 g_{a_0 K^+ K^-}$, where $\theta_p = 54.3^\circ$ is the "ideal" mixing angle. Taking into account that in the $s\bar{s}$ model the $g_{f_0 K^+ K^-} = \sqrt{2} g_{a_0 K^+ K^-}$ one gets $g_{a_0 \pi \eta} = 1.13 g_{f_0 K^+ K^-}$. The requirement, that the $\Gamma(a_0 \rightarrow \pi \eta) < 0.1 \text{ GeV}$, leads to the constraint $g_{f_0 K^+ K^-}^2/4\pi < 0.5 \text{ GeV}^2$. As it is seen from the Table I, in the $s\bar{s}$ model of the f_0 meson the branching ratio $BR(\phi \rightarrow \gamma(f_0 + \sigma) \rightarrow \gamma \pi \pi) \simeq 5 \cdot 10^{-5}$.

Notice again that the structure $f_0 = (u\bar{u} + d\bar{d})/\sqrt{2}$ with $R = 1/4 - 1/8$ is eliminated completely by the data on the $\pi\pi$ scattering. The data on the $\pi\pi$ scattering permit the ratio $R = g_{f_0 K^+ K^-}^2/g_{f_0 \pi^+ \pi^-}^2$ to range over the relatively large interval: $R = 1 - 20$. This interval is somewhat larger than expected previously, see [2,9,12]. This is due to the fact that previous experimental data pointed in favour of the narrow structure of the f_0 meson $\Gamma_{eff} \simeq 20 - 50 \text{ MeV}$ [36]. But now, in the decays of the J/ψ meson, in the reaction $J/\psi \rightarrow \phi f_0$ [40], the $f_0(980)$ -peak with $\Gamma_{eff} \simeq 80 \text{ MeV}$ is observed. The recent GAMS data on the reaction $\pi^- p \rightarrow \pi^0 \pi^0 n$ [32] at large momentum transfer show the $f_0(980)$ -peaks with $\Gamma_{eff} \simeq 50 \text{ MeV}$. In this reaction the E 852 Collaboration [41] also observes the $f_0(980)$ -peak with $\Gamma_{eff} = 61 \pm 18 \text{ MeV}$ at large momentum transfer.

In view of this, fitting the data on the $\pi\pi$ scattering, we considered also relatively small R ($R \simeq 1 - 5$) which leads to the $\Gamma_{eff} \lesssim 100 \text{ MeV}$.

The parameter set for the model of the $K\bar{K}$ molecule is tabulated in Table II and the illustrative graphics are shown in the Fig.5.

As seen in Table II, the data on the $\pi\pi$ scattering in the model of the $K\bar{K}$ molecule permit $\Gamma_{eff} = 10 - 30 \text{ MeV}$ which is likely for the bound $K\bar{K}$ state. Those values of the effective widths could be achieved with different parameters of the $K\bar{K}$ model. In this case, the branching ratios of the decays $\phi \rightarrow \gamma f_0 \rightarrow \gamma \pi \pi$ and $\phi \rightarrow \gamma(f_0 + \sigma) \rightarrow \gamma \pi \pi$ remain approximately the same and have the order of 10^{-5} .

Notice that the parameters obtained for the σ meson are in good agreement with those

discussed in the literature for the $\epsilon(1300)$ meson [36], currently known as $f_0(1300)$ [17] or $f_0(1370)$ [31] meson. Among all decay channels of this particle we have considered the main $\pi\pi$ only, $\Gamma_{2\pi}(m_\sigma) \simeq 300$ MeV. The channels $K\bar{K}$ and $\eta\eta$, as it was found, are relatively suppressed and change the parameters of the fitting very weakly. The influence of the 4π channel we analyzed separately and found that the account of it does not change our results essentially.

The decay width of the σ meson to 4π was approximated by the polynomial $m\Gamma_{4\pi}(m) = 0.32 \cdot (m - 0.7)(m - 0.6)$ so that $\Gamma_{4\pi}(m_\sigma = 1.5) = 150$ MeV and $\Gamma_{4\pi}(m = 0.7) = 0$. The analyses of the decay $f_0(1520) \rightarrow 4\pi$ shows that a such approximation is rather resonable, see [42]. The account of $im\Gamma_{4\pi}(m)$ in the propagator of the σ meson leads to the increasing of the coupling constant $g_{\sigma\pi\pi}$ and the σ meson become correspondingly wider $\Gamma_\sigma(m_\sigma) = \Gamma_{2\pi}(m_\sigma) + \Gamma_{4\pi}(m_\sigma) \simeq 550$ MeV. The branching ratios of the decays $\phi \rightarrow \gamma f_0 \rightarrow \gamma\pi\pi$ and $\phi \rightarrow \gamma(f_0 + \sigma) \rightarrow \gamma\pi\pi$ are changed by 8% and our main results, after taking into account the 4π channel, remain unchanged .

It is seen from the Tables I and II that the regions of the constants $g_{f_0 K^+ K^-}$ and $g_{f_0 \pi^+ \pi^-}$ in the four-quark model and in the model of the $K\bar{K}$ molecule overlap. It does not mean, of course, that in this case the models are the same since in the model of the $K\bar{K}$ molecule we consider the real intermediate states only in the the transitions caused by the resonance mixing due to the final state interaction. The suppression of the virtual states is typical for an extended molecule. At the same time, in the $q^2\bar{q}^2$ model we consider both the real and the virtual intermediate states.

B. $a_0(980)$ resonance.

As for the reaction $e^+e^- \rightarrow \gamma\pi^0\eta$ the similar analysis of the $\pi\eta$ scattering cannot be performed directly. But, our analysis of the final state interaction for the f_0 meson production show that the situation does not changed radically, in any case in the region $\omega < 100$ MeV. Hence, one can hope that the final state interaction in the $e^+e^- \rightarrow \gamma a_0 \rightarrow \gamma\pi\eta$ reaction will

not strongly affect the predictions in the region $\omega < 100$ MeV.

Recall that in the four-quark model the a_0 meson has a symbolic structure $a_0 = s\bar{s}(u\bar{u} - d\bar{d})/\sqrt{2}$ and the following relations are valid [2,9]:

$$\begin{aligned} g_{a_0 K^0 \bar{K}^0} &= -g_{a_0 K^+ K^-}; & g_{a_0 K^+ K^-} &= g_{f_0 K^+ K^-} \\ g_{a_0 \pi \eta} &= \sqrt{2} g_{a_0 K^+ K^-} \sin(\theta_p + \theta_{\eta\eta'}) = 0.85 g_{a_0 K^+ K^-} \\ g_{a_0 \pi \eta'} &= -\sqrt{2} g_{a_0 K^+ K^-} \cos(\theta_p + \theta_{\eta\eta'}) = -1.13 g_{a_0 K^+ K^-}. \end{aligned} \quad (43)$$

Based on the analysis of $\pi\pi$ scattering with regard to Eq.(43) we predict the quantities of the $BR(\phi \rightarrow \gamma a_0 \rightarrow \gamma \pi \eta)$ in the $q^2 \bar{q}^2$ model. The results are shown in the Table III.

In the propagator of the a_0 meson we consider the final width corrections corresponding the $\pi\eta, K\bar{K}, \pi\eta'$ channels, see Eq.(30). As is seen from Table III, in the $q^2 \bar{q}^2$ model of the a_0 meson the $BR(\phi \rightarrow \gamma a_0 \rightarrow \gamma \pi \eta) \simeq \cdot 10^{-4}$.

The last two lines in Table III relate to the $s\bar{s}$ model of the f_0 meson in which the a_0 meson is treated as a two-quark $(u\bar{u} - d\bar{d})/\sqrt{2}$ state. In this model [2,9]

$$\begin{aligned} g_{f_0 K^+ K^-} &= \sqrt{2} g_{a_0 K^+ K^-}; & g_{a_0 K^0 \bar{K}^0} &= -g_{a_0 K^+ K^-} \\ g_{a_0 \pi \eta} &= 2 g_{a_0 K^+ K^-} \cos(\theta_p + \theta_{\eta\eta'}) = 1.6 g_{a_0 K^+ K^-} \\ g_{a_0 \pi \eta'} &= 2 g_{a_0 K^+ K^-} \sin(\theta_p + \theta_{\eta\eta'}) = 1.2 g_{a_0 K^+ K^-}. \end{aligned} \quad (44)$$

Recall that in this case the $\phi \rightarrow \gamma a_0 \rightarrow \pi \eta$ decay is suppressed by the OZI rule, as discussed in the Introduction. The OZI suppression means that the real part of the $K^+ K^-$ loop is compensated by the virtual intermediate states $K^{*+} K^-$, $K^+ K^{*-}$, $K^{*+} K^{*-}$ and so on. Because there is a real two-particle intermediate $K^+ K^-$ state the OZI rule violating imaginary part of the decay amplitude is relatively large [9]. In view of this, we consider the imaginary part of the $\phi \rightarrow \gamma a_0(q\bar{q})$ decay amplitude only. As one can see from Table III in the two-quark model of the a_0 meson the $BR(\phi \rightarrow \gamma a_0 \rightarrow \gamma \pi \eta) \simeq 8 \cdot 10^{-6}$.

In the model of the $K\bar{K}$ molecule the relations $g_{a_0 K^0 \bar{K}^0} = -g_{a_0 K^+ K^-}$ and $g_{a_0 K^+ K^-} = g_{f_0 K^+ K^-}$ are valid, in this case $BR(\phi \rightarrow \gamma a_0 \rightarrow \gamma \pi \eta) \sim 10^{-5}$. The results are listed in Table IV.

C. Metamorphosis of the $a_0(980)$ and $f_0(980)$ resonances.

In this section we would like to discuss the definition of the scalar resonance effective widths listed in the tables.

According to the current view, away from the thresholds of the reactions the production amplitude of the scalar resonance has the form $A = g_i g_j / (s - m_R^2 + im_R \Gamma)$, where the quantities g_i, g_j are the constants. So, the form of the resonance defined by Breit-Wigner formulae has a universal form and is described by the two parameters: the mass and the width. Most resonances, especially narrow ones, satisfy this condition of universality and are adequately described by the Breit-Wigner form. But, such a simple situation is not always true.

The availability of the channels in the immediate vicinity of the resonance point, with which the resonance strongly couples, leads to energy-dependent g_i, g_j quantities. Also, the denominator becomes an intricate function of the energy, see Eq.(29), Eq.(30), in which both the real and imaginary parts vary rapidly. This leads to a considerable distortion of the simple Breit-Wigner formulae, see [2,30,43]. The property of the universality is lost in this case, the resonance form, in particular the visible width, depends on the specific production mode of the resonance.

This phenomena can be brightly demonstrated by the example of the scalar a_0 and f_0 resonances.

In the peripheral production of the a_0 meson, for example, in the reaction $\pi^- p \rightarrow \pi^0 \eta n$, the mass spectrum of the $\pi\eta$ system is determined by the expression

$$\frac{dN_{\pi\eta}}{dm} \sim \frac{m^2 \Gamma_{a_0\pi\eta}(m)}{|D_{a_0}(m)|^2}, \quad (45)$$

where m is the mass of the $\pi\eta$ system. In Table III the effective widths corresponding to this distribution are listed (in the four-quark model $g_{a_0\pi\eta} = 0.85g_{a_0K^-K^+}$). In the $e^+e^- \rightarrow \phi \rightarrow \gamma a_0 \rightarrow \gamma\pi\eta$ reaction the mass spectrum of the $\pi\eta$ system is determined by the expression

$$\frac{d\sigma_\phi}{dm} = \frac{\alpha^2 m}{16\pi s^3} \left(\frac{m_\phi^2}{f_\phi} \right)^2 \frac{|g(m)|^2}{|D_\phi(s)|^2} (s - m^2) \sqrt{1 - \frac{4m_\pi^2}{m^2} \left(c + \frac{c^3}{3} \right)} \left| \frac{g_{a_0 K^+ K^-} - g_{a_0 \pi^0 \eta}}{D_{a_0}(m)} \right|^2 H(s, \omega_{min}). \quad (46)$$

For the constant listed in the Table III, at $g_{a_0 K^+ K^-}^2/4\pi > 1 \text{ GeV}^2$ in the $q^2 \bar{q}^2$ model, the visible width of the mass spectrum of the $\pi\eta$ system is twice as large as the effective one determined by Eq.(45). For illustration those two spectrum are depicted together in Fig.6(a).

So, considering the specific resonance production mechanism (the one charge kaon loop production) widens the spectrum twice as much.

Notice that such an effect is especially strong at the large coupling constants, i.e. in the four-quark model. With the coupling constant decrease the effect dies out, for example, at the $g_{a_0 K^+ K^-}^2/4\pi = 0.72 \text{ GeV}^2$, as it is seen in Fig.6(b), the width of the mass spectrum of the $\pi\eta$ system is one and a half as large as the one determined by Eq.(45), and at the $g_{a_0 K^+ K^-}^2/4\pi = 0.3 \text{ GeV}^2$ this effect is negligible.

For the f_0 resonance the situation is somewhat the same with the difference that the width of the resonance depends on the free parameter R . At the $R = 1 - 3$ the resonance is relatively wide and the distinction between the widths of the $\pi\pi$ mass spectra in the $e^+e^- \rightarrow \phi \rightarrow \gamma\pi\pi$ reaction and in the distribution

$$\frac{dN_{\pi\pi}}{dm} \sim \frac{m^2 \Gamma_{f_0 \pi\pi}(m)}{|D_{f_0}(m)|^2}, \quad (47)$$

is strong, see Fig.7(a). The phase and the inelasticity are shown in Fig.8 in this case . At large R , when the effective resonance width $\Gamma_{eff} \sim 30 \text{ MeV}$, the difference is not so noticeable. The illustrative picture is shown in the Fig.7(b).

Notice that when analyzing the definite processes it is needed to take into account the initial and final state interactions. Let us consider the f_0 production in the J/ψ decay, where the peak with the visible width $\Gamma \simeq 80 \text{ MeV}$ is observed [40]. The spectrum of the $\pi\pi$ system is determined by the expression

$$\frac{dN_{\pi\pi}}{dm} \sim \frac{m^2 \Gamma_{f_0 \pi\pi}(m)}{|D_{f_0}(m)|^2} \cdot \left| \frac{D_\sigma(m) + (1 + \chi) \Pi_{f_0 \sigma}(m) + \chi (g_{\sigma \pi\pi} / g_{f_0 \pi\pi}) D_{f_0}(m)}{D_\sigma(m) - \Pi_{f_0 \sigma}^2 / D_{f_0}(m)} \right|^2, \quad (48)$$

where χ is a relative weight of the σ meson production. For the width of Eq.(48) to be the visible width $\Gamma \simeq 80$ MeV one needs to take not only the effective width $\Gamma_{eff} \simeq 80$ MeV, but to consider $\chi = 1$ as well. If one considers that the σ meson is not produced in the initial state, i.e. $\chi = 0$, but is produced as a result of the mixing with the f_0 meson only in the final state, then the visible width of the spectrum Eq.(48) is equal to $\Gamma \simeq 40$ MeV.

V. CONCLUSION.

We have shown that the vector meson contribution $e^+e^- \rightarrow V^0 \rightarrow \pi^0 V^0 \rightarrow \gamma \pi^0 \pi^0(\eta)$ to the $e^+e^- \rightarrow \gamma \pi^0 \pi^0(\eta)$ reaction is negligible in comparison with the scalar $f_0(a_0)$ meson one $e^+e^- \rightarrow \phi \rightarrow \gamma f_0(a_0) \rightarrow \gamma \pi^0 \pi^0(\eta)$ for $BR(\phi \rightarrow \gamma f_0(a_0))$ greater than $5 \cdot 10^{-6}(10^{-5})$, in the photon energy region less than 100 MeV.

Based on the two-channel analysis of the $\pi\pi$ scattering we predict for the $\phi \rightarrow \gamma(f_0 + \sigma) \rightarrow \gamma\pi\pi$ reaction in the region $0.7 < m < m_\phi$ that the $BR(\phi \rightarrow \gamma(f_0 + \sigma) \rightarrow \gamma\pi\pi) \sim 10^{-4}$ and $BR(\phi \rightarrow \gamma a_0 \rightarrow \gamma\pi\eta) \sim 10^{-4}$ in the $q^2\bar{q}^2$ model.

In the model of the $K\bar{K}$ molecule we get $BR(\phi \rightarrow \gamma(f_0 + \sigma) \rightarrow \gamma\pi\pi) \sim 10^{-5}$ and $BR(\phi \rightarrow \gamma a_0 \rightarrow \gamma\pi\eta) \sim 10^{-5}$.

In the two-quark $s\bar{s}$ model of the f_0 meson we obtain $BR(\phi \rightarrow \gamma(f_0 + \sigma) \rightarrow \gamma\pi\pi) \simeq 5 \cdot 10^{-5}$ and taking into account the imaginary part of the decay amplitude only, as the main one, we get $BR(\phi \rightarrow \gamma a_0(q\bar{q}) \rightarrow \gamma\pi\eta) \simeq 8 \cdot 10^{-6}$.

Notice that the variants listed in the Table I describe equally well the $\pi\pi$ scattering data, see, for example, Fig.4 and Fig.8. We could not find the parameters at which the data on the $\pi\pi$ scattering are described well but the $BR(\phi \rightarrow \gamma(f_0 + \sigma) \rightarrow \gamma\pi\pi)$ is less than 10^{-5} . Or, more precisely, we could get $BR(\phi \rightarrow \gamma(f_0 + \sigma) \rightarrow \gamma\pi\pi) \simeq 10^{-5}$, only if we dropped out the real part of the K^+K^- loop in the $\phi \rightarrow K^+K^- \rightarrow \gamma(f_0 + \sigma)$ decay amplitude, otherwise we got $BR(\phi \rightarrow \gamma(f_0 + \sigma) \rightarrow \gamma\pi\pi) \gtrsim 4.5 \cdot 10^{-5}$, see Table I. Forgetting the possible models, one can say that from the $\pi\pi$ scattering results $BR(\phi \rightarrow \gamma(f_0 + \sigma) \rightarrow \gamma\pi\pi) \gtrsim 10^{-5}$, that is enormous for the suppressed by the OZI rule decay.

We gratefully acknowledge discussions with M. Arpagaus, S.I. Eidelman and J.A Thompson.

This research was supported in part by the Russian Foundation for Basic Research, grants 94-02-05 188, 96-02-00 548 and INTAS-94-3986.

VI. APPENDIX.

The function $f_\rho(m)$, taking into account the interference of the identical pions, see Fig.1, has the following integral presentation

$$f_\rho(m) = 1 - \frac{3}{8m^2p^2\omega} \int_{m_\pi}^{\tilde{m}} \text{Re} \left(\frac{D_\rho(m)}{D_\rho(z)} \right) \{ y[(s - 2m^2)(E_+ - py) - 2\omega(E_+ - py)^2 - (49) \\ - 2mm_\pi^2] + \frac{p}{2}(z^2 + m^2 - s)(1 - y^2) \} z dz,$$

where

$$p = \sqrt{(s - (m - m_\pi)^2)(s - (m + m_\pi)^2)}/2m, \quad \omega = (m^2 - m_\pi^2)/2m, \quad (50) \\ E_+ = (s - m_\pi^2 - m^2)/2m, \quad z^2 = m_\pi^2 + 2\omega(E_+ - py), \quad \tilde{m}^2 = 2m_\pi^2 + 2m_\phi\omega - m^2.$$

The function $f_\omega(m)$ is resulted from (49) by replacement $D_\rho(m) \rightarrow D_\omega(m)$.

REFERENCES

- [1] L. Montanet, Rep. Prog. Phys. **46**, 337 (1983).
- [2] N.N. Achasov, S.A. Devyanin and G.N. Shestakov, Usp. Fiz. Nauk. **142**, 361 (1984).
- [3] F.E. Close, Rep. Prog. Phys. **51**, 833 (1988).
- [4] L.G. Landsberg, Usp. Fiz. Nauk **160**,1 (1990).
- [5] N.N. Achasov, Nucl. Phys. B (Proc. Suppl.) **21**, 189 (1991).
- [6] N.N. Achasov and G.N. Shestakov, Usp. Fiz. Nauk **161**, No 6, 53 (1991).
- [7] R.L. Jaffe, Phys. Rev. **D15**, 267, 281 (1977).
- [8] J. Weinstein and N. Isgur, Phys. Rev. **D41**, 2236 (1990).
- [9] N.N. Achasov and V.N.Ivanchenko, Nucl. Phys. **B315**,465 (1989),
Preprint INP 87-129 (1987), Novosibirsk.
- [10] F.E. Close, N. Isgur and S. Kumano, Nucl. Phys. **B 389** (1993) 513.
N. Brown and F. Close, *The Second DAΦNE Physics Handbook*, Vol. II, edited by L. Maiani, G. Pancheri, N. Paver, dei Laboratory Nazionali di Frascati, Frascati, Italy (May 1995), p. 649.
- [11] N.N. Achasov, V.V. Gubin and V.I.Shevchenko, to be published in Phys. Rev. D, (hep-ph/9605245).
- [12] N.N. Achasov, *The Second DAΦNE Physics Handbook*, Vol. II, edited by L. Maiani, G. Pancheri, N. Paver, dei Laboratory Nazionali di Frascati, Frascati, Italy (May 1995), p. 671.
- [13] N.A. Törnqvist Phys. Rev. Lett., **49**, 624 (1982).
- [14] N.A. Törnqvist, Z. Phys. **C 68** 647 (1995).
- [15] A. Billoire et al., Phys. Lett. **B 80** 381 (1979).

- [16] G. Eigen, *Proc. the XXIV International Conference on High Energy Physics*, Munich, August 4-10, 1988, p. 590, Springer-Verlag, Eds. R. Kotthaus and J.H. Kuhn.
- [17] Particle Data Group, *Phys. Rev. D* **50** 1468, 1469 (1994).
- [18] R.R. Akhmetshin et al., preprint Budker INP 95-62, 1995.
- [19] M.N. Achasov et al., preprint Budker INP 96-47, 1996.
- [20] N.N. Achasov, V.V. Gubin and E.P. Solodov, *Phys. Rev. D* **55** 2627 (1997), (hep-ph/9610282).
- [21] S.I. Dolinski et al., *Phys. Rep. C* **202** 99 (1991).
- [22] A. Bramon, A. Grau, G. Pancheri, *The DAΦNE Physics Handbook*, V.II, /Eds L.Maiani, G.Pancheri and N.Paver, P.487.;
- [23] J. Lee-Franzini, W. Kim, P.J. Franzini, *The DAΦNE Physics Handbook*, V.II /Eds L.Maiani, G.Pancheri and N.Paver, P.513.
J. Lee-Franzini, W. Kim, P.J. Franzini, preprint LNF-92/026 (R), 9 Aprile, 1992.
G. Colangelo, P.J. Franzini, preprint LNF-92/058 (P), 22 Giugno, 1992.
- [24] X. He et al., *Phys. Rev. D* **31**, 2356 (1985).
- [25] A. Bramon, A. Grau, G. Pancheri, *The Second DAΦNE Physics Handbook*, V.II, /Eds L.Maiani, G.Pancheri and N.Paver, P.477.
- [26] N.N. Achasov and G.N. Shestakov, *Phys. Rev. D* **49** 5779 (1994).
- [27] N.N. Achasov, S.A. Devyanin and G.N. Shestakov, *Z. Phys. C* **22** 53 (1984).
- [28] E. Kuraev and V.S. Fadin, *Yad. Fiz.* **41**, 733 (1985).
- [29] N.N. Achasov and V.V. Gubin, *Phys. Lett. B* **363** 106 (1995).
- [30] N.N. Achasov, S.A. Devyanin and G.N. Shestakov, *Yad. Fiz.* **33** 1337 (1981).

- [31] Particle Data Group, Phys. Rev. **D 54** 27, 28 (1996).
- [32] D. Alde et al., Z. Phys. **C 66** 375 (1995)
A.A. Kondashov et al., *Proc. 27th Intern. Conf. on High Energy Physics*, Glasgow (1994)
1407
Yu.D. Prokoshkin et al., Physics-Doklady **342** 473 (1995)
A.A. Kondashov et al., Preprint IHEP 95-137, Protvino (1995)
- [33] A.R. Dzierba, *Workshop on Physics and Detectors for DAΦNE'95*, Eds. R. Baldini, F. Bossi, G. Capon, G. Pancheri, Frascati, April 1995, p.99.
- [34] D. Morgan and M.R. Pennington, Phys. Lett. **B 258** 444 (1991),
Phys. Lett. **B 269** 477 (1991) (E).
- [35] V.V. Anisovich, Phys. Lett. **B 364** 195 (1995).
- [36] Particle Data Group, Rev. Mod. Phys. **56** S19 (1984).
- [37] B. Hyams et al., Nucl. Phys. **B 64** 134 (1973).
- [38] P. Estabrooks and A.D. Martin, Nucl. Phys. **B 79** 301 (1974).
- [39] A.D. Martin, E.N. Ozmutlu, E.J. Squires, Nucl. Phys. **B 121** 514 (1977).
- [40] A. Falvard et al., Phys. Rev. **D 38** 2706 (1988).
- [41] B.B. Brabson, *The 6th International Conference on Hadron Spectroscopy*, Eds. M.C. Birse, G.D. Lafferty and J.A. McGovern, Manchester, UK, July 1995, p. 494.
- [42] N.N. Achasov and G.N. Shestakov, Phys. Rev. **D 53**, 3559 (1996).
- [43] N.N. Achasov and G.N. Shestakov, Z. Phys. **C 41**, 309 (1988).

FIGURES

FIG. 1. The diagrams of the background to the $e^+e^- \rightarrow \gamma f_0 \rightarrow \gamma \pi^0 \pi^0$ process in the vector dominance model .

FIG. 2. The diagrams of the background to the $e^+e^- \rightarrow \gamma a_0 \rightarrow \gamma \pi^0 \eta$ process in the vector dominance model.

FIG. 3. The symbolic diagrams of the $e^+e^- \rightarrow \phi \rightarrow \gamma(f_0 + \sigma) \rightarrow \gamma \pi \pi$ process with regard to the f_0 and σ mesons mixing.

FIG. 4. The results of fitting in the $q^2 \bar{q}^2$ model for the parameters: $\theta = 60^\circ$, $R = 2.0$, $g_{f_0 K^+ K^-}^2/4\pi = 0.72 \text{ GeV}^2$, $g_{\sigma \pi \pi}^2/4\pi = 1.76 \text{ GeV}^2$, $C_{f_0 \sigma} = -0.17 \text{ GeV}^2$, $m_\sigma = 1.47 \text{ GeV}$, $m_{f_0} = 0.98 \text{ GeV}$. The effective width of the f_0 meson $\Gamma_{eff} \simeq 60 \text{ MeV}$. The $BR_{f_0+\sigma}(BR_{f_0}) = 3 \cdot BR(\phi \rightarrow \gamma(f_0 + \sigma) \rightarrow \gamma \pi^0 \pi^0)(3 \cdot BR(\phi \rightarrow \gamma f_0 \rightarrow \gamma \pi^0 \pi^0)) = 1.18(1.43) \cdot 10^{-4}$ at $\omega < 250 \text{ MeV}$ and $BR_{f_0+\sigma}(BR_{f_0}) = 0.63(0.6) \cdot 10^{-4}$ at $\omega < 100 \text{ MeV}$. (a) The inelasticity $\eta_{L=0}^{I=0}$. (b) The phase $\delta_{L=0}^{I=0}$. (c) The spectrum of the differential cross section $d\sigma(e^+e^- \rightarrow \gamma(f_0 + \sigma) \rightarrow \gamma \pi^0 \pi^0)/d\omega$ with mixing of the f_0 and σ mesons, see Eq.(26). The dashed line is the spectrum of the f_0 meson without mixing with the σ meson. The cut of the angle of the photon direction $c = 0.66$ reduces the cross section by 43%.

FIG. 5. The results of fitting in the model of the $K\bar{K}$ molecule for the parameters: $\theta = 58^\circ$, $\Gamma_0 = 0.1 \text{ GeV}$, $g_{f_0 K^+ K^-}^2/4\pi = 0.6 \text{ GeV}^2$, $g_{\sigma \pi \pi}^2/4\pi = 2.15 \text{ GeV}^2$, $m_\sigma = 1.48 \text{ GeV}$, $m_{f_0} = 0.98 \text{ GeV}$. The effective width of the f_0 meson $\Gamma_{eff} \simeq 30 \text{ MeV}$. The $BR_{f_0+\sigma}(BR_{f_0}) = 3 \cdot BR(\phi \rightarrow \gamma(f_0 + \sigma) \rightarrow \gamma \pi^0 \pi^0)(3 \cdot BR(\phi \rightarrow \gamma f_0 \rightarrow \gamma \pi^0 \pi^0)) = 1.21(1.53) \cdot 10^{-5}$ at $\omega < 250 \text{ MeV}$ and $BR_{f_0+\sigma}(BR_{f_0}) = 0.91(1.13) \cdot 10^{-5}$ at $\omega < 100 \text{ MeV}$. (a) The inelasticity $\eta_{L=0}^{I=0}$. (b) The phase $\delta_{L=0}^{I=0}$. (c) The spectrum of the differential cross section $d\sigma(e^+e^- \rightarrow \gamma(f_0 + \sigma) \rightarrow \gamma \pi^0 \pi^0)/d\omega$ with the mixing of the f_0 and σ mesons, see Eq.(26). The dashed line is the spectrum of the f_0 meson without mixing with the σ meson. The cut of the angle of the photon direction $c = 0.66$ reduces the cross section by 43%.

FIG. 6. The mass spectrum of the $\pi\eta$ system in the $e^+e^- \rightarrow \phi \rightarrow \gamma a_0 \rightarrow \gamma\pi\eta$ reaction in the $q^2\bar{q}^2$ model. The dashed line is the spectrum $dN/dm \sim m^2\Gamma_{\pi\eta}/|D_{a_0}(m)|^2$. (a) The constant $g_{a_0K^+K^-}^2/4\pi = 1.47 \text{ GeV}^2$, $m_{a_0} = 0.98 \text{ GeV}$. The effective width of the a_0 meson $\Gamma_{eff} \simeq 60 \text{ MeV}$. (b) The constant $g_{a_0K^+K^-}^2/4\pi = 0.72 \text{ GeV}^2$, $m_{a_0} = 0.985 \text{ GeV}$. The effective width of the a_0 meson $\Gamma_{eff} \simeq 34 \text{ MeV}$.

FIG. 7. The mass spectrum of the $\pi\pi$ system in the $e^+e^- \rightarrow \phi \rightarrow \gamma(f_0 + \sigma) \rightarrow \gamma\pi\pi$ reaction in the $q^2\bar{q}^2$ model. The dotted line is the mass spectrum without mixing with the σ meson. The dashed line is the spectrum $dN/dm \sim m^2\Gamma_{\pi\pi}/|D_{f_0}(m)|^2$. (a) $\theta = 45^\circ$, $R = 2$, $g_{f_0K^+K^-}^2/4\pi = 1.47 \text{ GeV}^2$, $g_{\sigma\pi\pi}^2/4\pi = 1.76 \text{ GeV}^2$, $C_{f_0\sigma} = -0.31 \text{ GeV}^2$, $m_\sigma = 1.38 \text{ GeV}$, $m_{f_0} = 0.985 \text{ GeV}$. The effective width of the f_0 meson $\Gamma_{eff} \simeq 85 \text{ MeV}$. (b) $\theta = 60^\circ$, $R = 8$, $g_{f_0K^+K^-}^2/4\pi = 2.25 \text{ GeV}^2$, $g_{\sigma\pi\pi}^2/4\pi = 1.76 \text{ GeV}^2$, $C_{f_0\sigma} = -0.31 \text{ GeV}^2$, $m_\sigma = 1.47 \text{ GeV}$, $m_{f_0} = 0.98 \text{ GeV}$. The effective width of the f_0 meson $\Gamma_{eff} \simeq 25 \text{ MeV}$.

FIG. 8. The phase and inelasticity of the $\pi\pi$ scattering for the same parametres as in Fig.7(a).

TABLES

TABLE I. The results in the $q^2\bar{q}^2$ model. In the three last lines the parameters and results are listed for the $s\bar{s}$ model of the f_0 meson. All dimensional quantities are shown in units of GeV or GeV^2 . The details are described in the Sec.IV .

θ	R	$\frac{g_{f_0^{K+K-}}^2}{4\pi}$	$\frac{g_{\pi\pi\pi}^2}{4\pi}$	m_σ	$-C_{f_0\sigma}$	Γ_{eff}	$BR_{f_0+\sigma}(BR_{f_0}) \cdot 10^4$	$BR_{f_0+\sigma}(BR_{f_0}) \cdot 10^4; \omega < 0.1$	m_{f_0}
45°	2.0	1.47	1.76	1.38	0.31	0.095	1.05(0.95)	0.71(0.76)	0.98
45°	2.0	1.47	1.76	1.38	0.31	0.100	1.21(1.14)	0.81(0.91)	0.975
45°	2.0	1.47	1.76	1.38	0.31	0.110	2.36(3.0)	0.9(0.83)	0.970
45°	2.0	1.47	1.76	1.38	0.31	0.085	1.67(2.32)	0.59(0.68)	0.985
50°	2.0	1.47	1.76	1.4	0.28	0.090	1.41(2.00)	0.49(0.59)	0.990
60°	2.0	0.72	1.76	1.47	0.17	0.060	1.18(1.43)	0.63(0.6)	0.98
60°	2.0	0.72	1.76	1.47	0.17	0.055	1.01(1.27)	0.52(0.54)	0.985
60°	2.0	0.72	1.76	1.47	0.17	0.060	0.81(1.09)	0.39(0.45)	0.990
60°	2.0	0.72	1.76	1.47	0.17	0.070	1.34(1.56)	0.73(0.66)	0.975
55°	4.0	1.47	2.1	1.47	0.31	0.042	1.6(2.05)	0.76(0.97)	0.980
50°	4.0	4.25	1.76	1.47	0.31	0.061	2.9(3.8)	1.24(1.22)	0.980
60°	8.0	2.25	1.76	1.47	0.31	0.025	2.74(3.36)	1.0(0.79)	0.98
60°	8.0	2.25	1.91	1.49	0.31	0.017	2.39(3.04)	0.75(0.74)	0.985
60°	8.0	2.25	1.91	1.49	0.31	0.030	3.06(3.63)	1.22(0.83)	0.975
60°	9.0	0.72	2.0	1.48	0.29	0.015	1.11(1.43)	0.68(0.6)	0.98
60°	9.0	0.72	2.0	1.48	0.29	0.010	0.97(1.27)	0.54(0.54)	0.985
60°	9.0	0.72	2.0	1.48	0.29	0.005	0.82(1.1)	0.38(0.45)	0.990
60°	15.0	1.47	2.0	1.48	0.35	0.010	1.94(2.57)	1.02(0.74)	0.98
55°	4.0	0.3	2.2	1.45	0.29	0.02	0.45(0.52)	0.29(0.33)	0.985
50°	2.0	0.3	2.2	1.43	0.29	0.04	0.52(0.6)	0.27(0.38)	0.98
50°	1.0	0.3	2.2	1.43	0.29	0.06	0.52(0.6)	0.24(0.31)	0.98

TABLE II. The parameters and results in the model of the $K\bar{K}$ molecule. The $BR_{f_0+\sigma}(BR_{f_0}) = 3 \cdot BR(\phi \rightarrow \gamma(f_0 + \sigma) \rightarrow \gamma\pi^0\pi^0)(3 \cdot BR(\phi \rightarrow \gamma f_0 \rightarrow \gamma\pi^0\pi^0))$ are listed for the region $\omega < 250 \text{ MeV}$ ($0.7 < m < m_\phi$). All demensional quantities are shown in units of GeV or GeV^2 . The details are described in the Sec.IV.

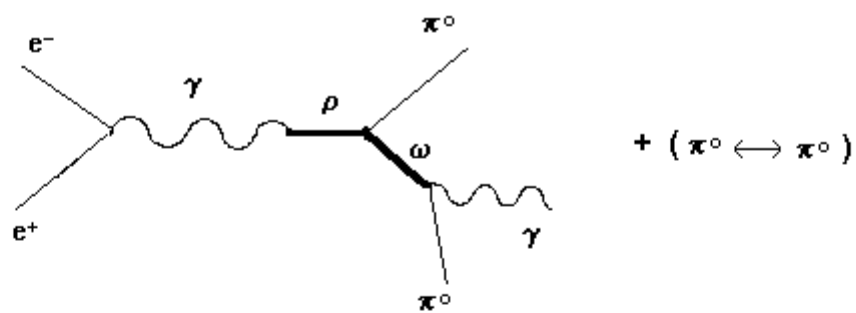
θ	Γ_0	$\frac{g_{f_0 K^+ K^-}^2}{4\pi}$	$\frac{g_{\sigma\pi\pi}^2}{4\pi}$	m_σ	Γ_{eff}	$BR_{f_0+\sigma}(BR_{f_0}) \cdot 10^5$	$BR_{f_0+\sigma}(BR_{f_0}) \cdot 10^5; \omega < 0.1$	m_{f_0}
58°	0.10	0.6	2.15	1.48	0.03	1.21(1.53)	0.91(1.13)	0.98
58°	0.10	0.6	2.15	1.48	0.02	1.00(1.34)	0.73(0.98)	0.985
58°	0.10	0.6	2.15	1.48	0.015	0.78(1.11)	0.55(0.79)	0.99
58°	0.10	0.6	2.15	1.48	0.035	1.41(1.7)	1.1(1.25)	0.975
60°	0.05	0.6	2.1	1.5	0.01	1.82(2.66)	1.53(2.27)	0.985

TABLE III. The branching ratios of the $\phi \rightarrow \gamma a_0 \rightarrow \pi \eta$ decay in the $q^2 \bar{q}^2$ model. In the two last lines the parameters and results are listed for the $s\bar{s}$ model of the f_0 meson. All dimensional quantities are shown in units of GeV or GeV^2 . The details are described in the Sec.IV .

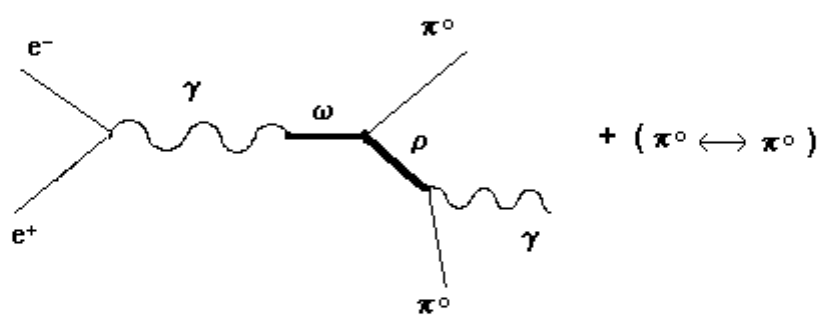
$\frac{g_{a_0 K^+ K^-}^2}{4\pi}$	Γ_{eff}	$BR_{a_0} \cdot 10^4; \omega < 0.25$	$BR_{a_0} \cdot 10^4; \omega < 0.1$	m_{a_0}
1.47	0.056	1.78	0.86	0.98
1.47	0.062	2.0	0.96	0.975
1.47	0.067	2.22	1.05	0.97
1.47	0.047	1.535	0.74	0.985
1.47	0.051	1.25	0.58	0.99
0.72	0.039	1.05	0.65	0.98
0.72	0.034	0.9	0.55	0.985
0.72	0.037	0.72	0.42	0.99
0.72	0.043	1.19	0.75	0.975
2.25	0.067	2.3	0.96	0.98
2.25	0.056	2.0	0.83	0.985
2.25	0.075	2.6	1.06	0.975
1.78	0.04	1.78	0.86	0.98
0.3	0.049	0.079	0.074	0.985
0.3	0.05	0.085	0.08	0.98

TABLE IV. The branching ratios of the $\phi \rightarrow \gamma a_0 \rightarrow \pi\eta$ decay in the model of the $K\bar{K}$ molecule. All dimensional quantities are shown in units of GeV or GeV^2 . The details are described in the Sec.IV .

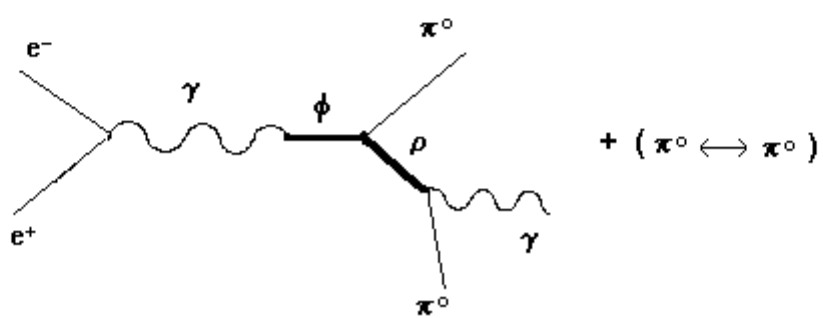
$\frac{g_{a_0 K^+ K^-}^2}{4\pi}$	Γ_0	Γ_{eff}	$BR_{a_0} \cdot 10^5; \omega < 0.25$	$BR_{a_0} \cdot 10^5; \omega < 0.1$	m_{a_0}
0.6	0.05	0.027	0.85	0.73	0.975
0.6	0.05	0.023	0.74	0.64	0.98
0.6	0.05	0.020	0.60	0.51	0.985
0.6	0.05	0.023	0.43	0.35	0.99



a)



b)



c)

Fig.1

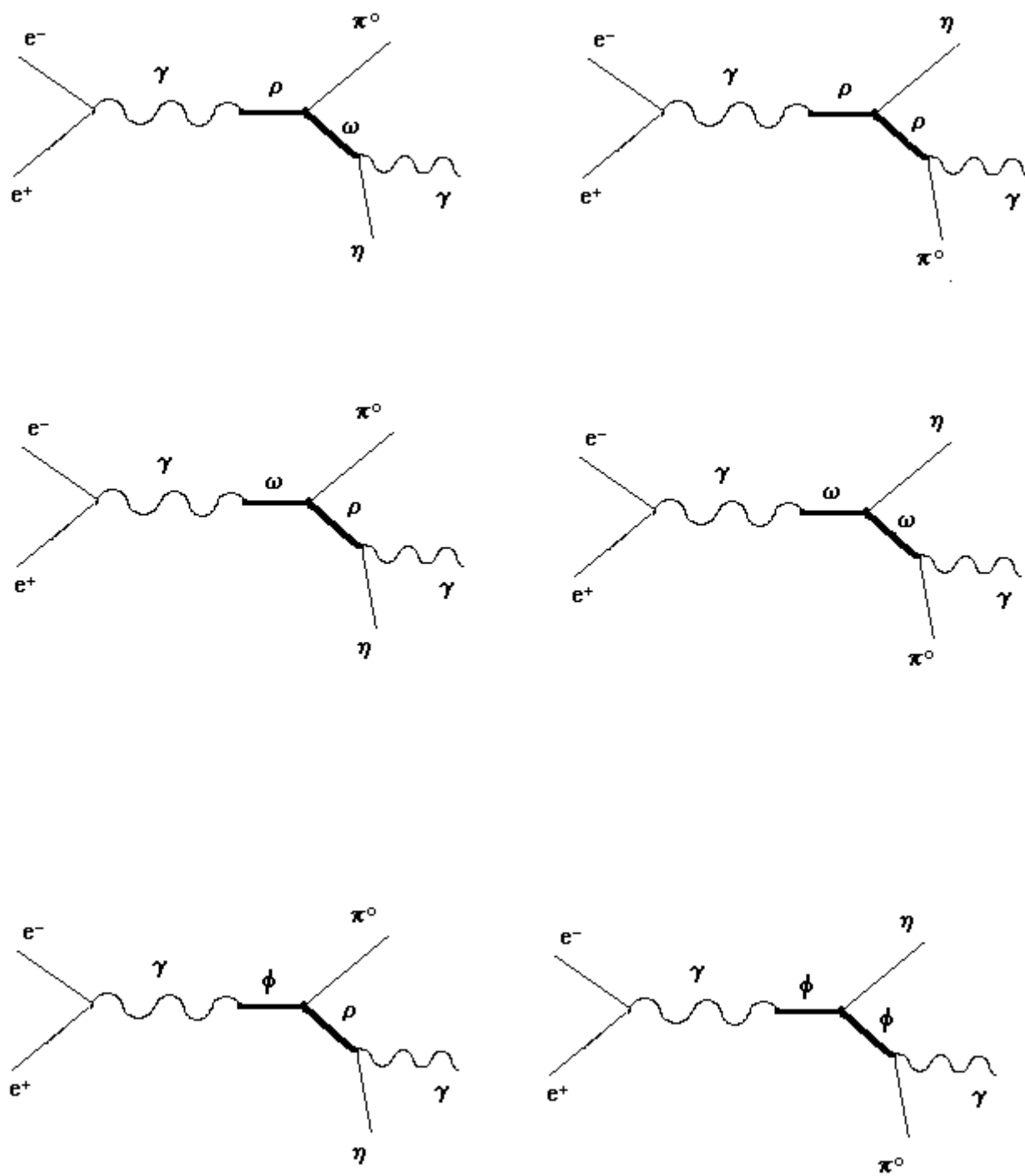


Fig.2

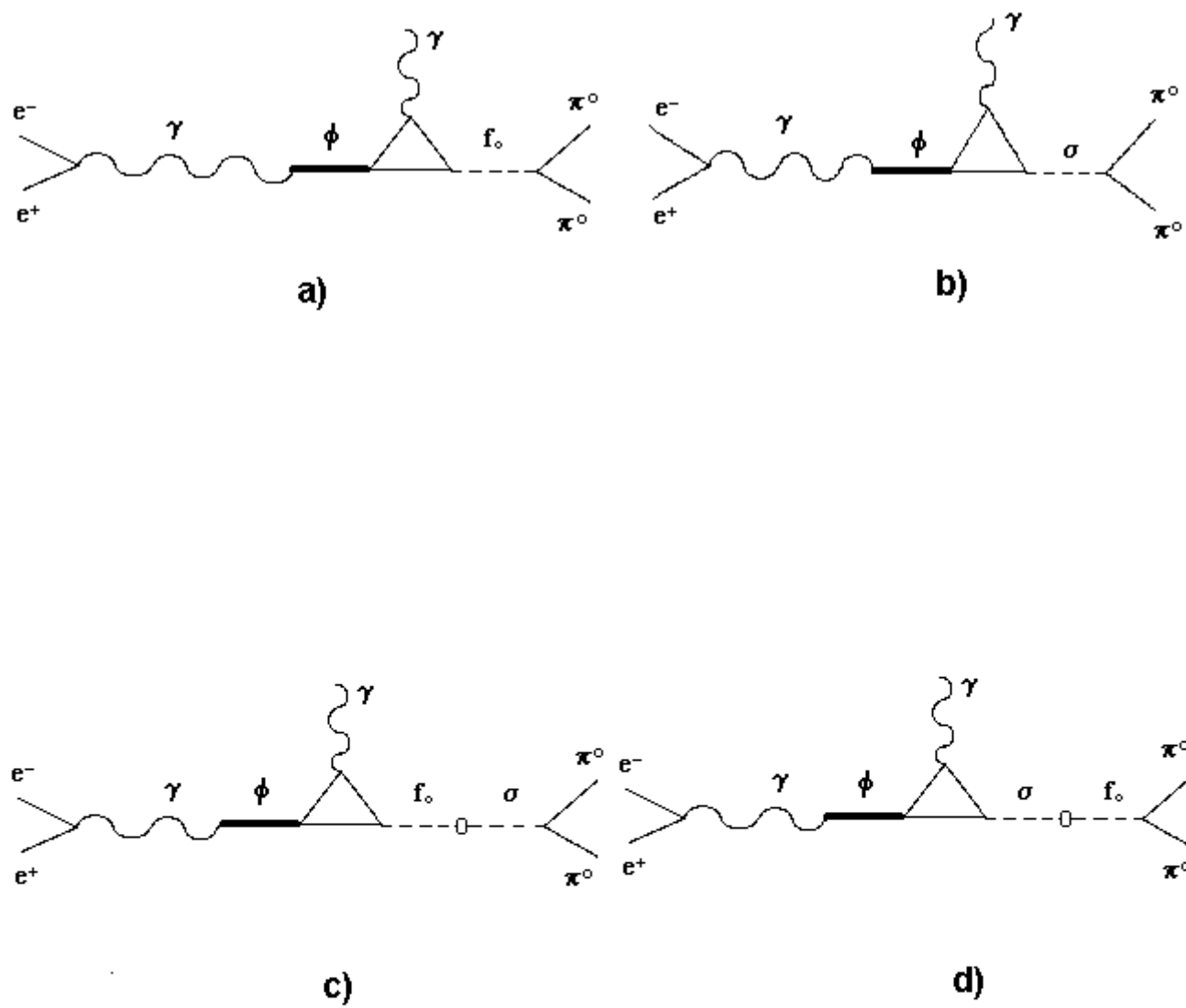


Fig. 3

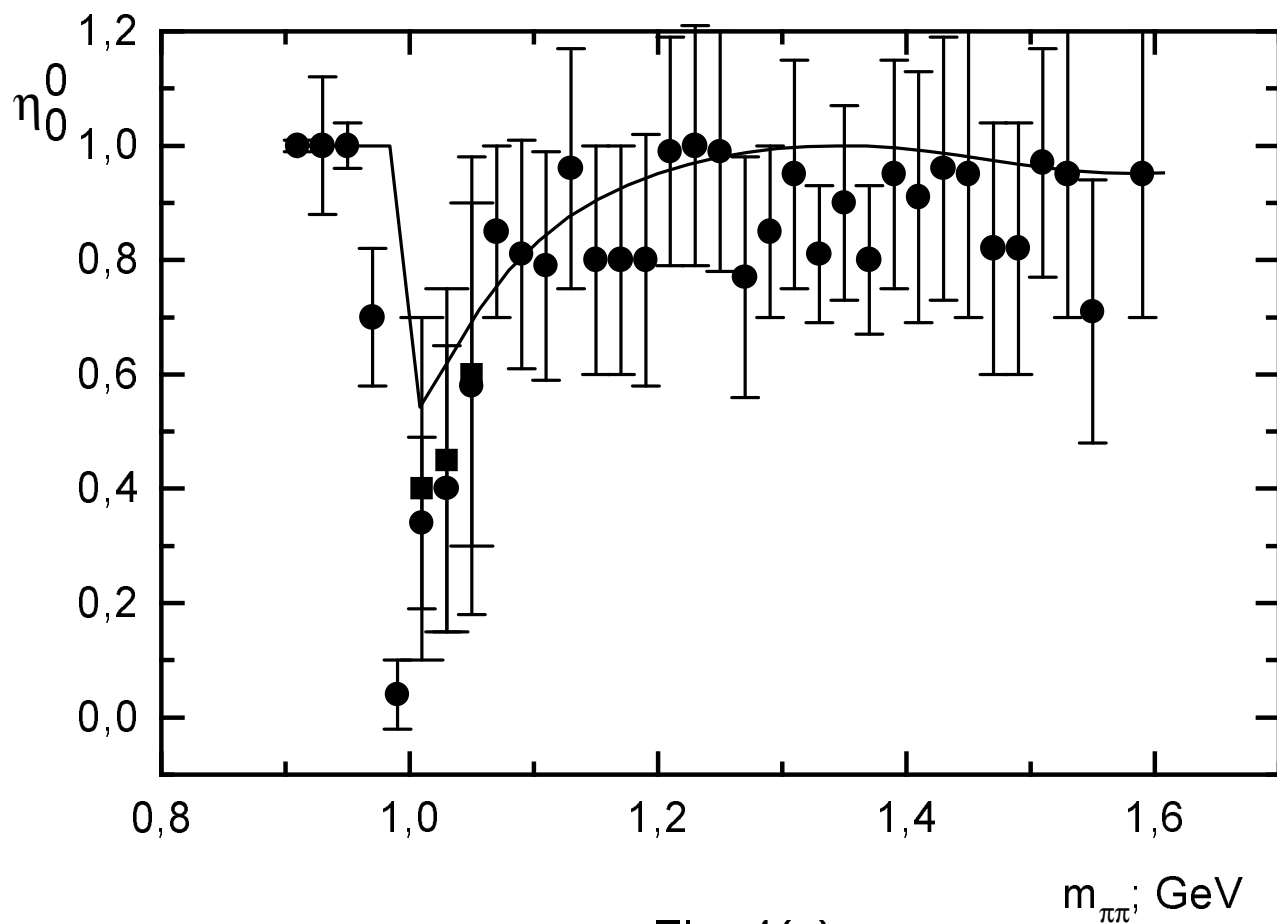


Fig. 4(a)

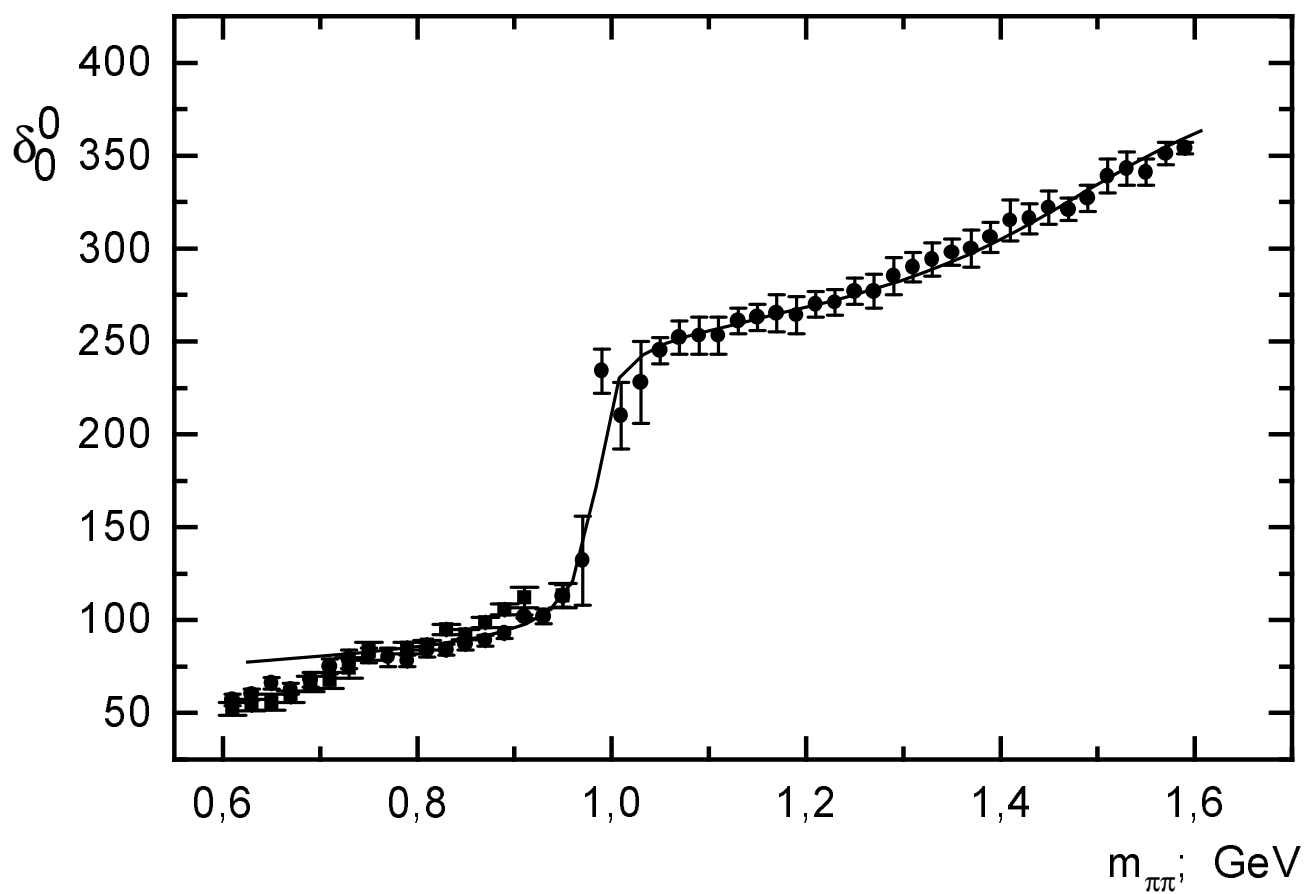


Fig. 4(b)

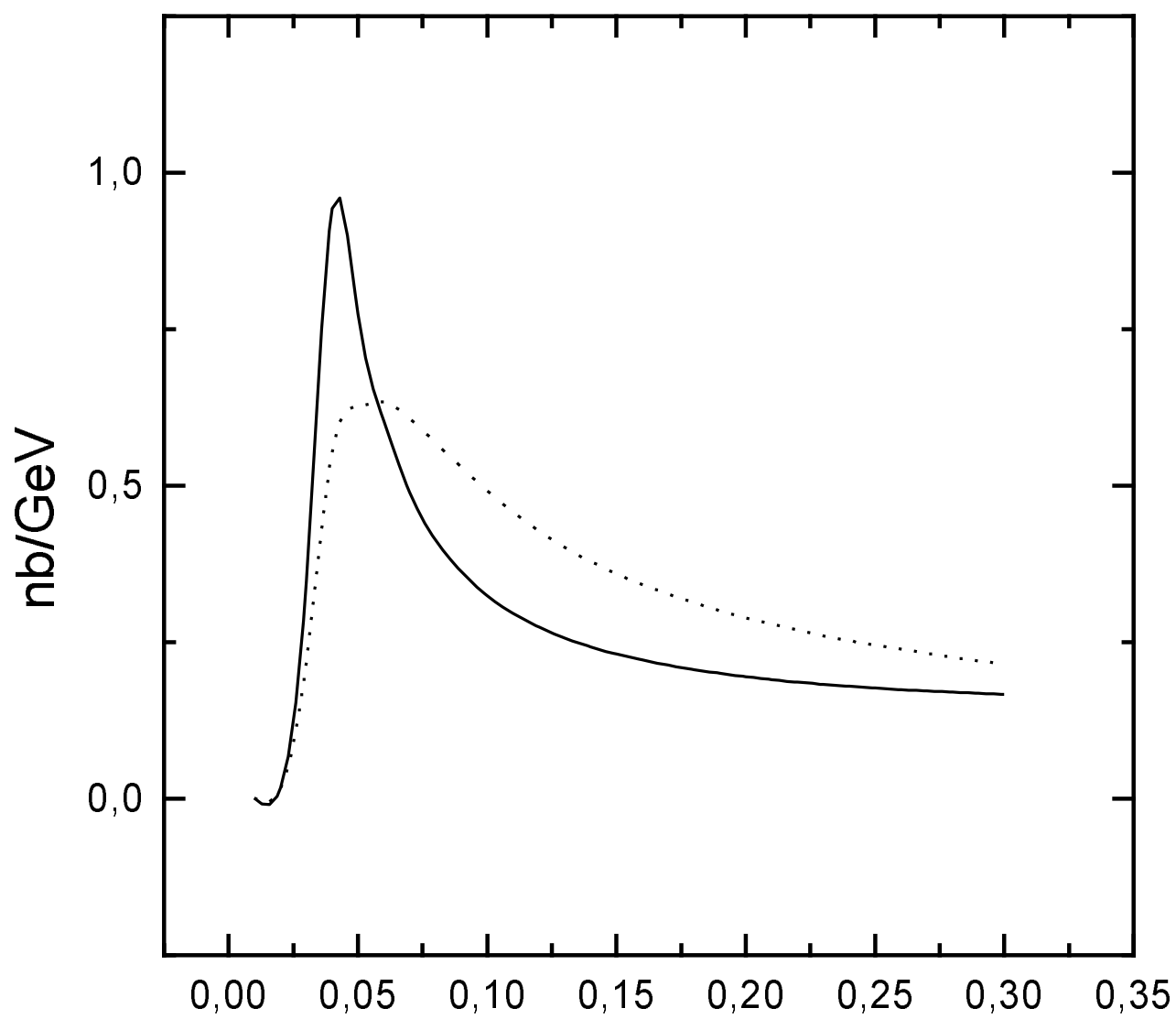


Fig. 4(c)

$\omega; GeV$

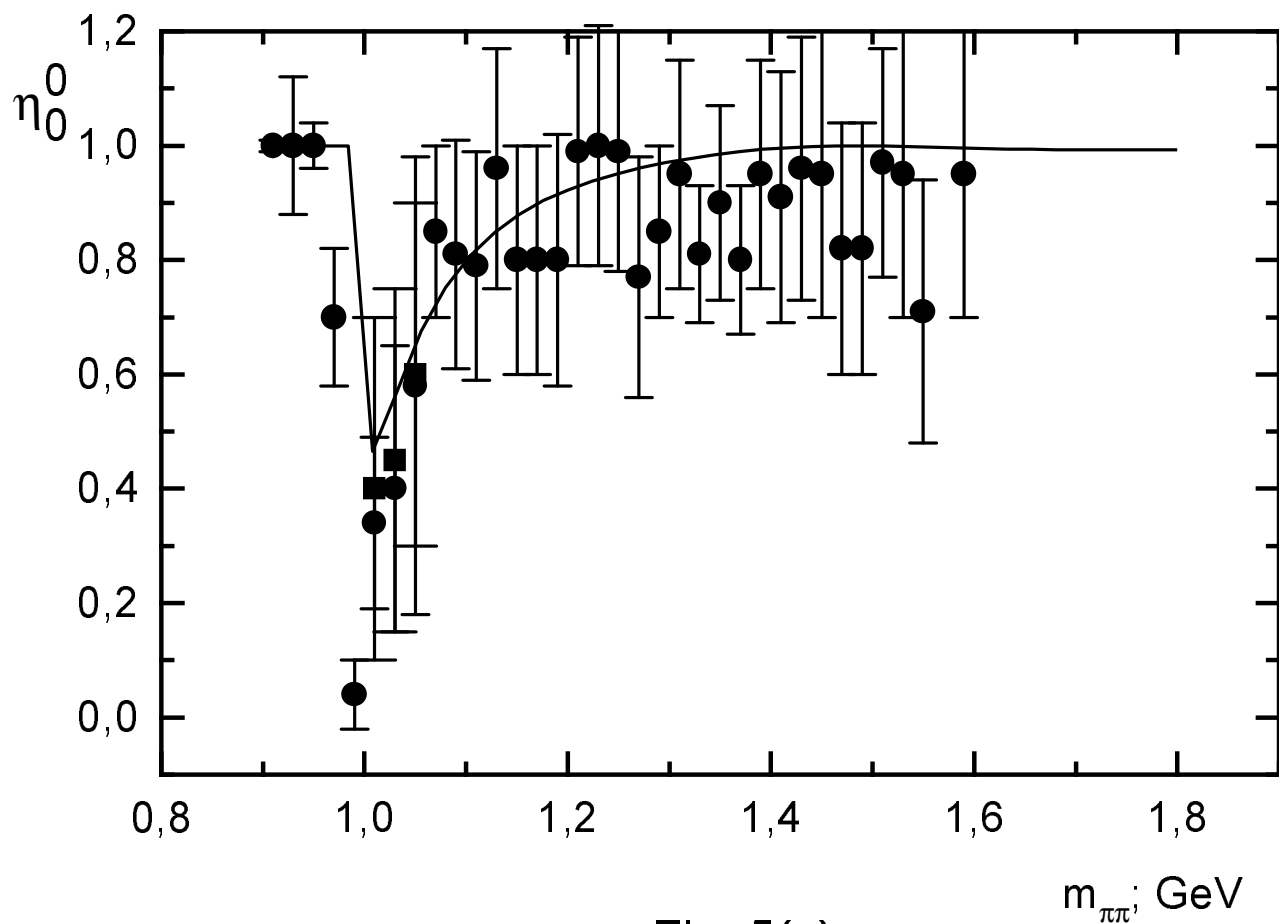


Fig. 5(a)

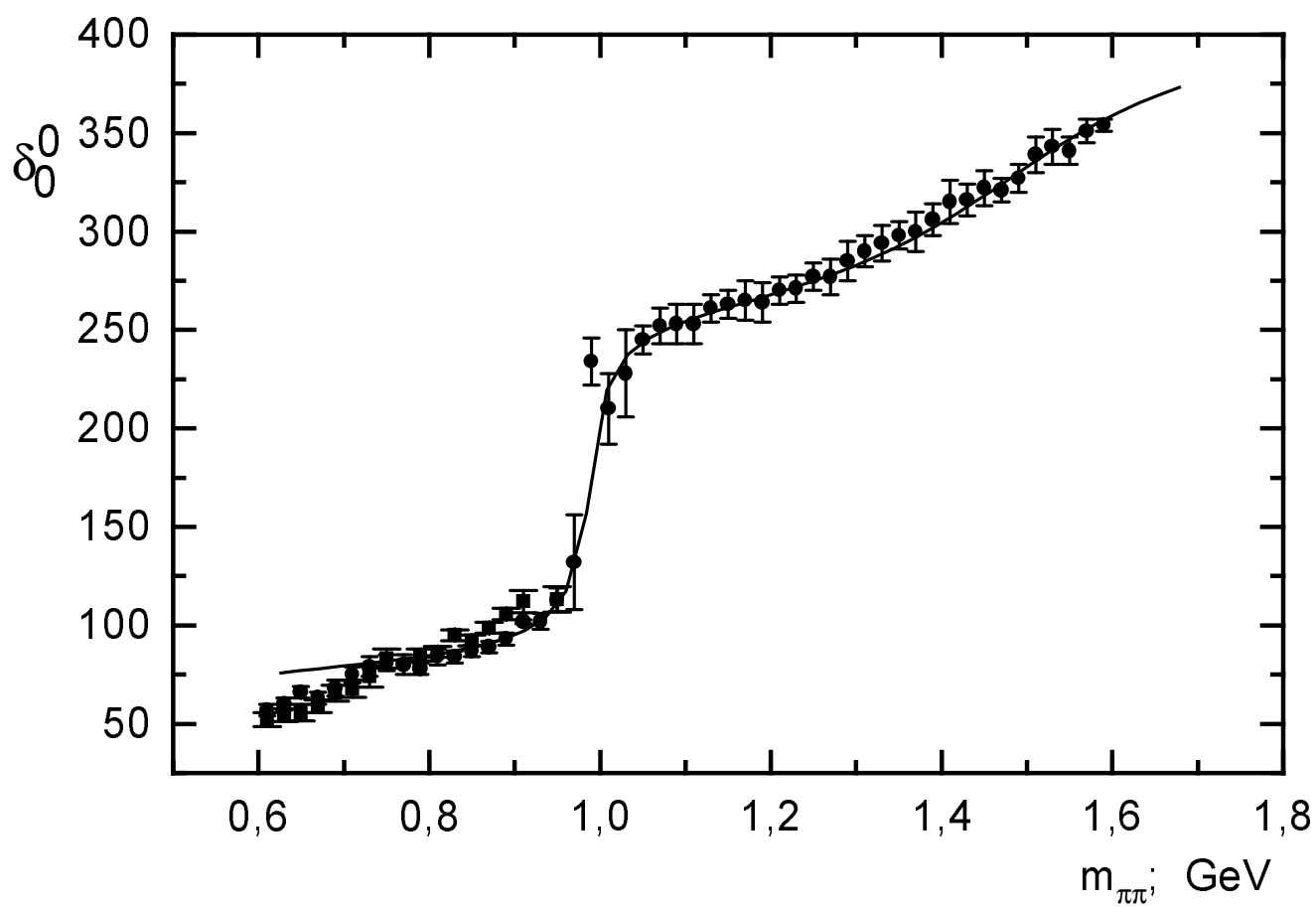


Fig. 5(b)

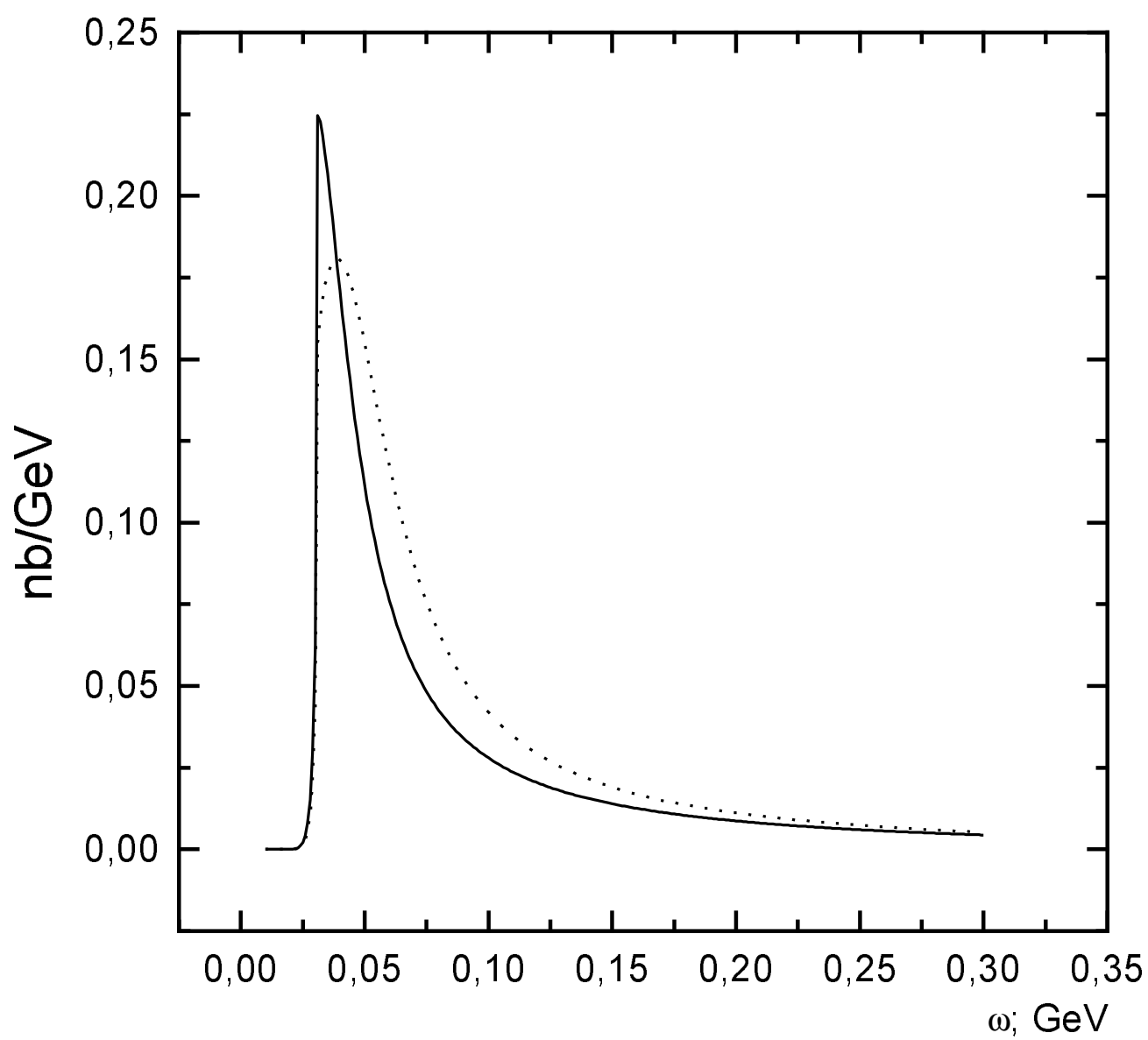


Fig. 5(c)

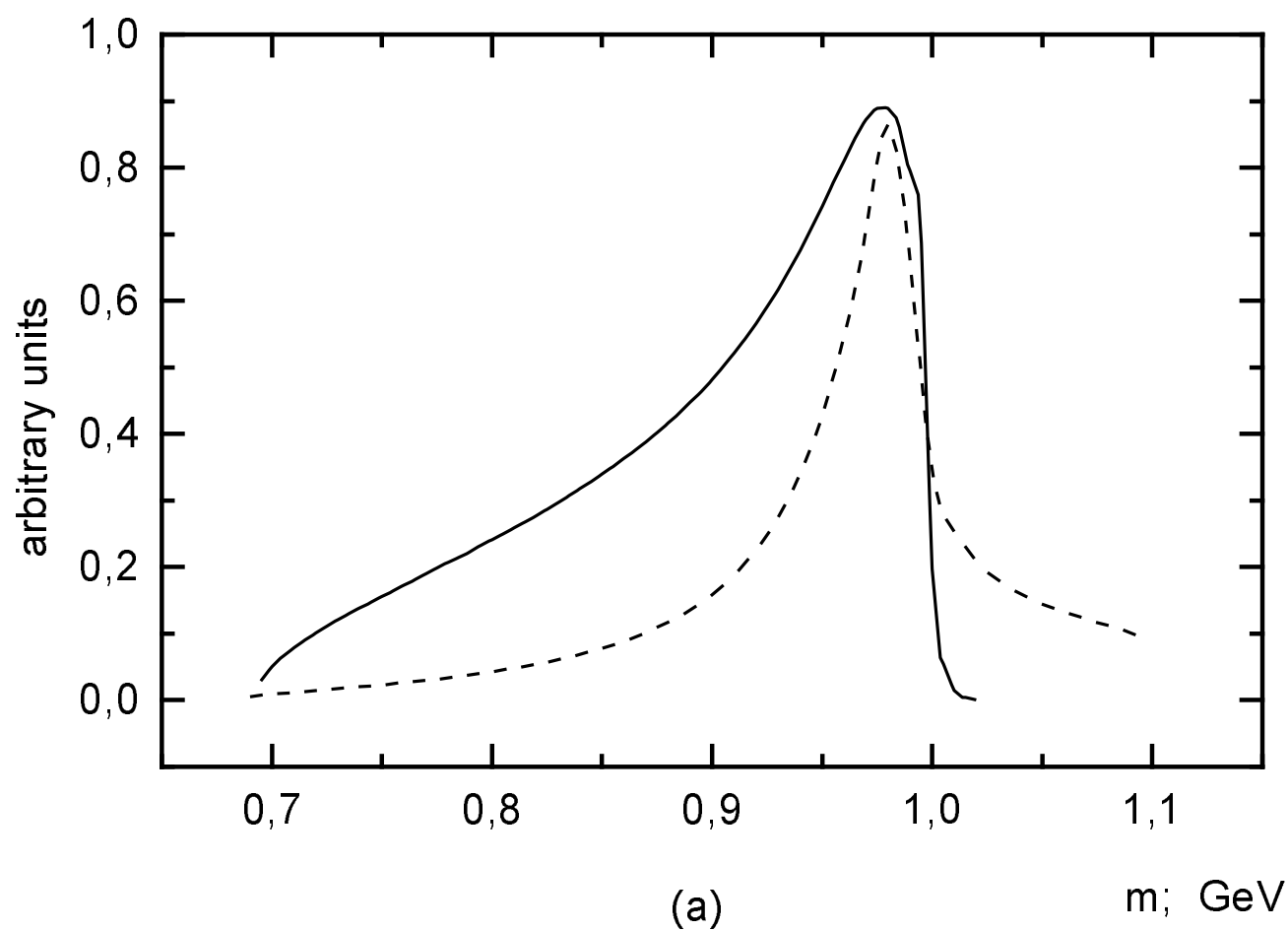
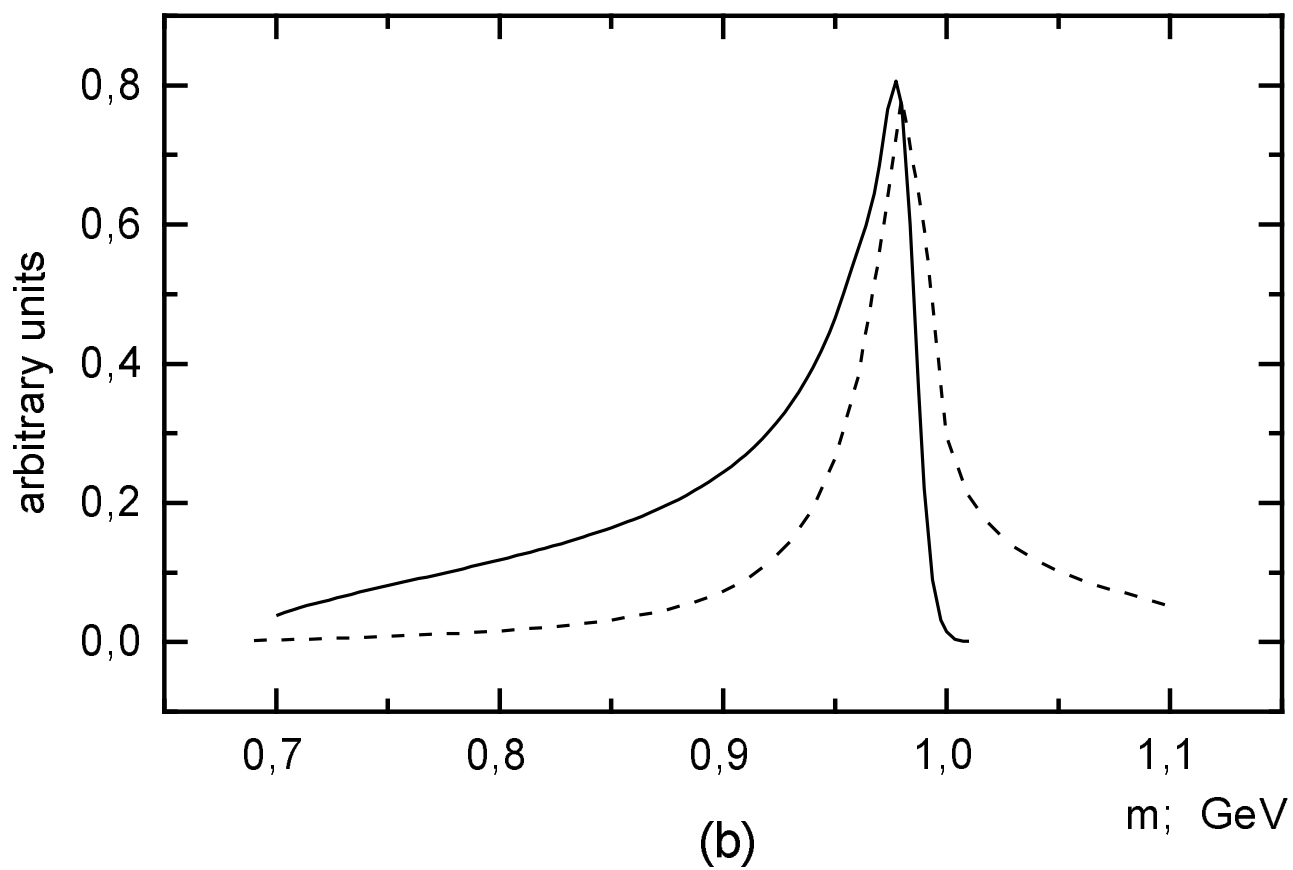


Fig. 6

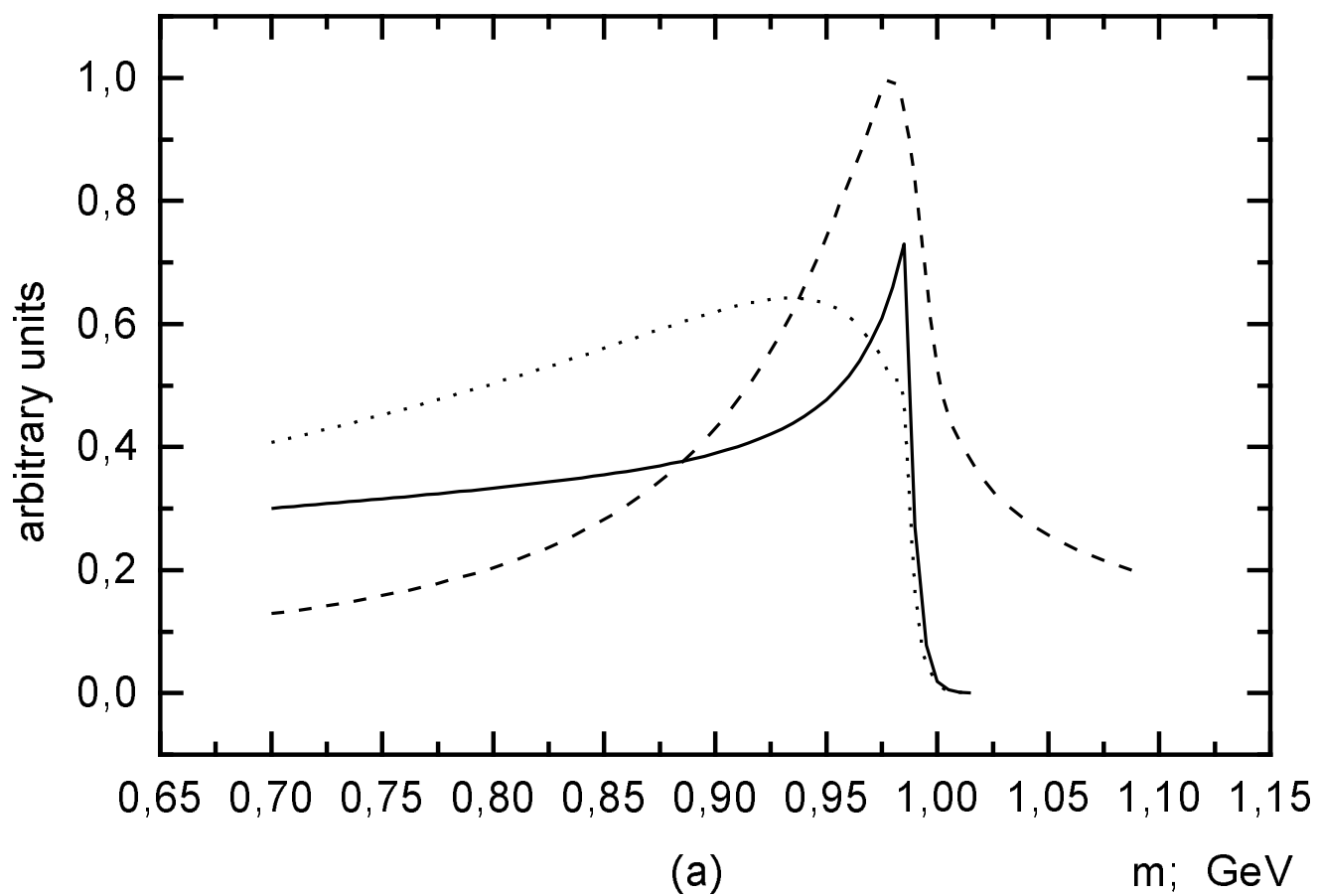
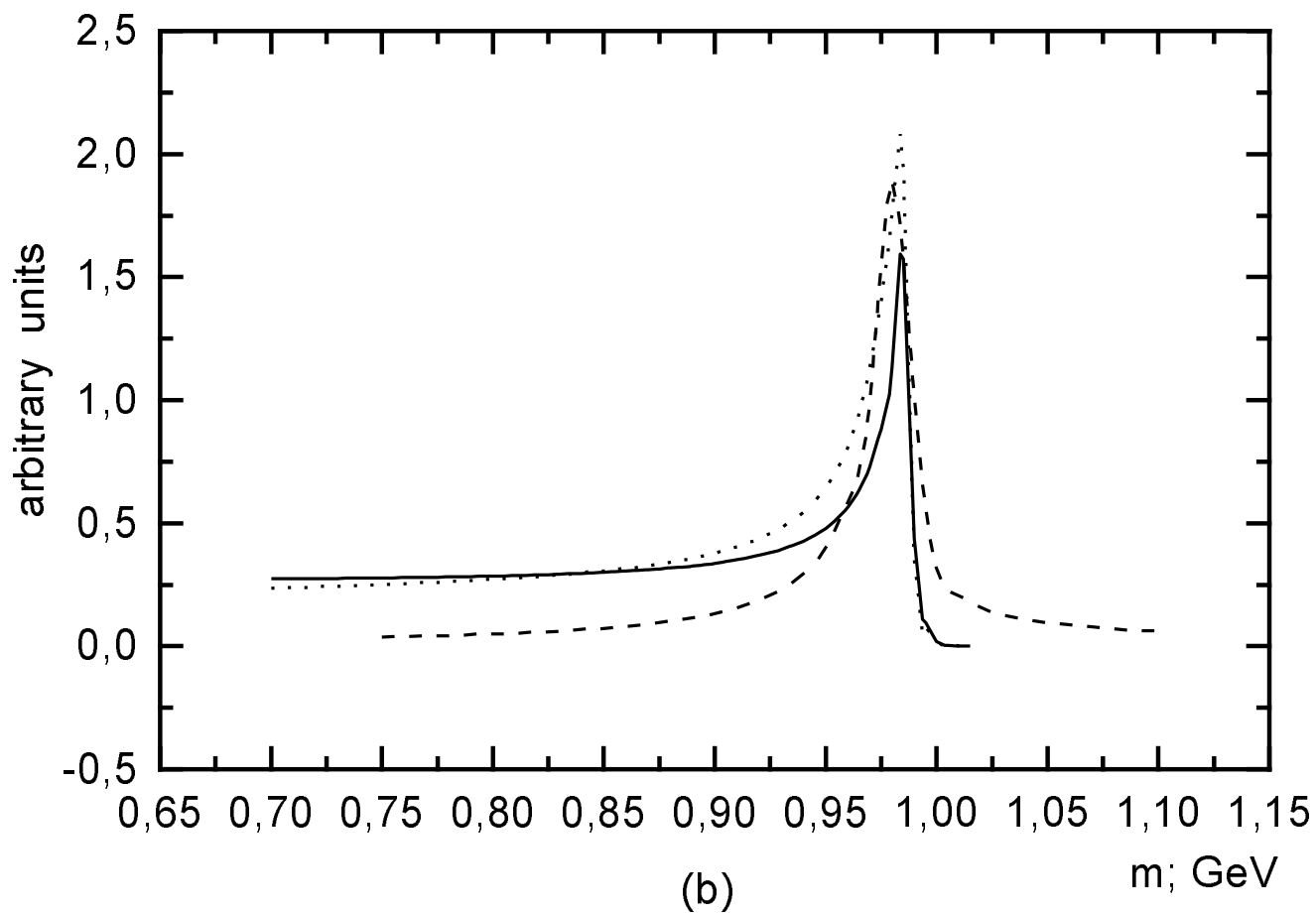


Fig. 7

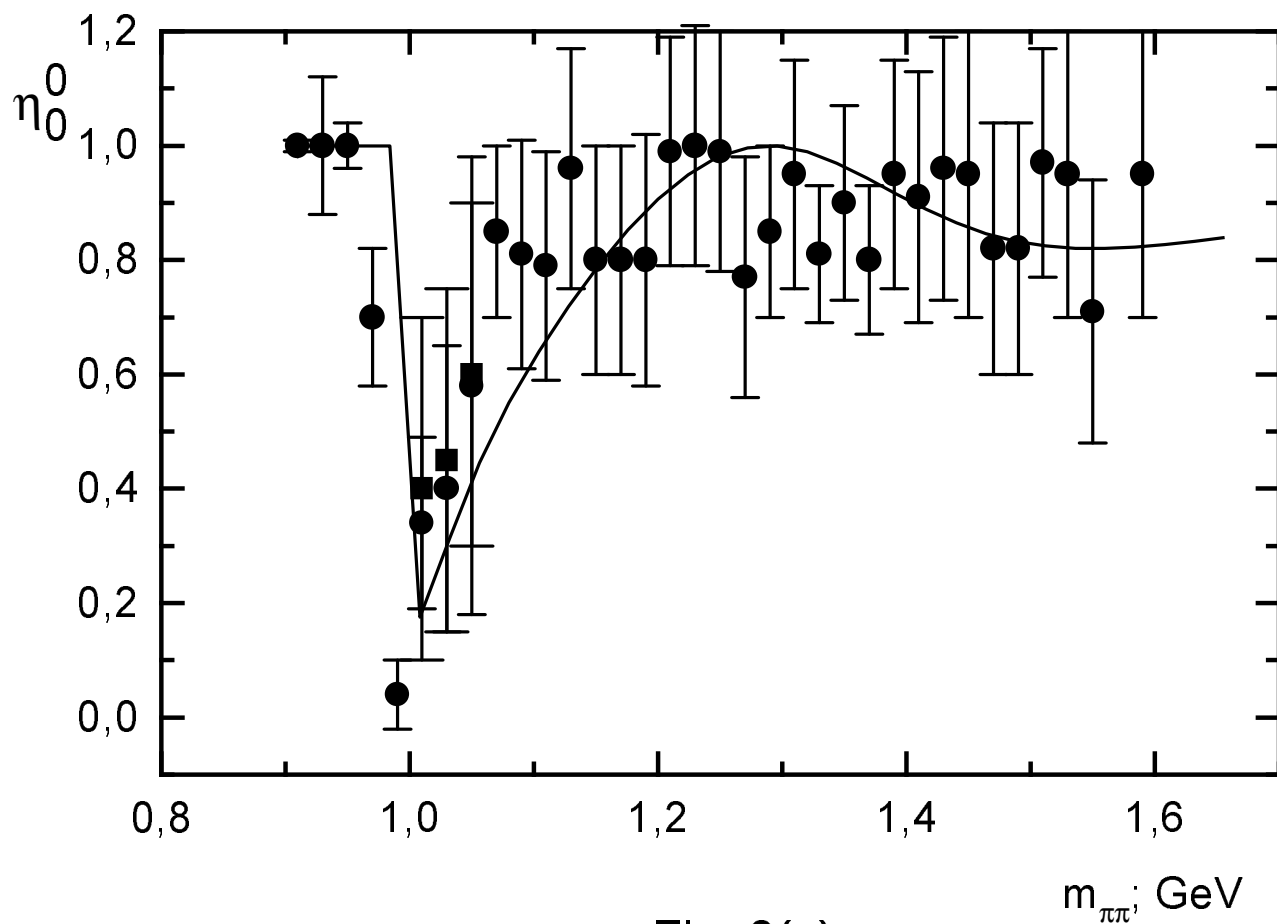


Fig. 8(a)

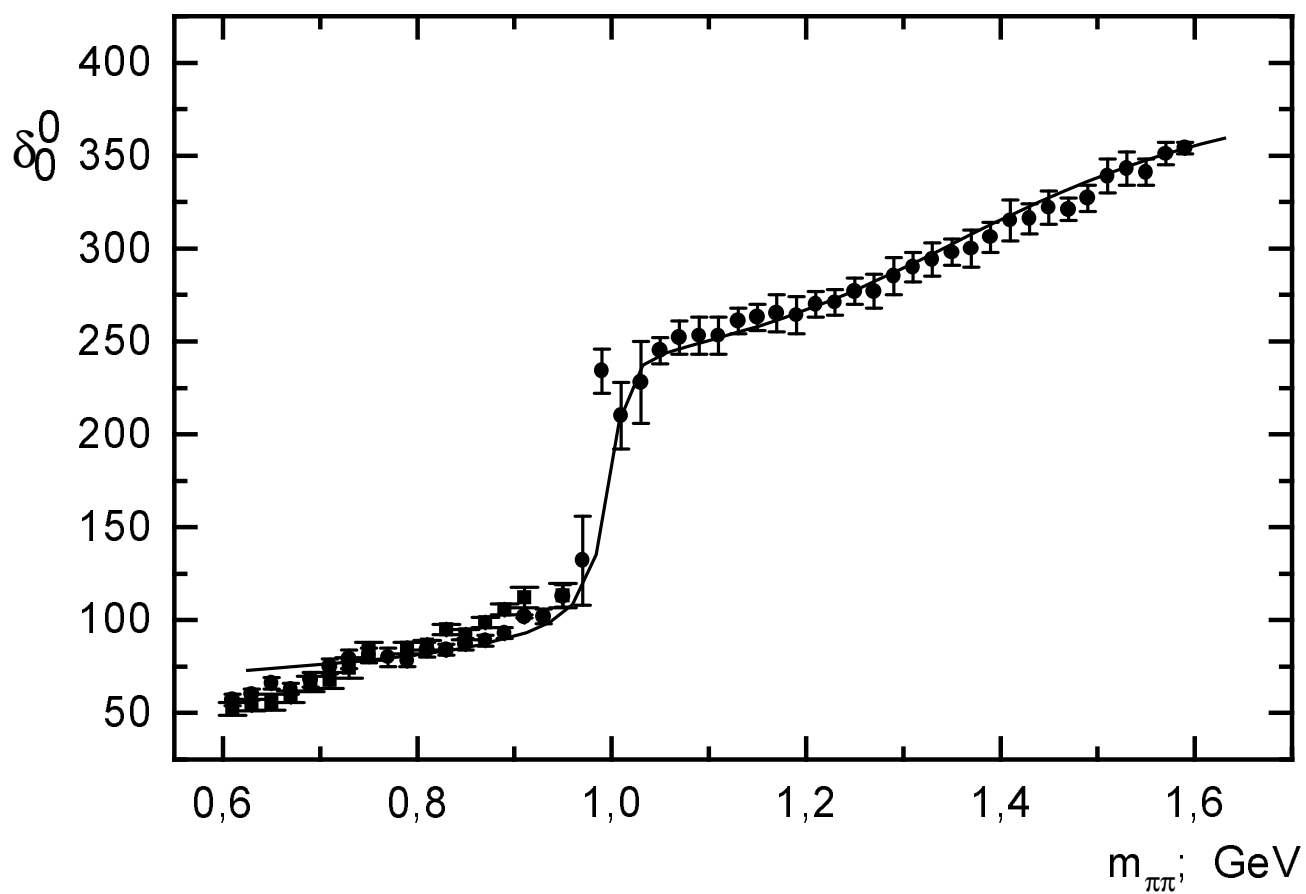


Fig. 8(b)